

1 **MicroRNAs of the miR-17~92 family maintain adipose tissue**
2 **macrophage homeostasis by sustaining IL-10 expression**

3

4 **Xiang Zhang^{1,2,3}, Jianguo Liu⁴, Li Wu^{1,2,3}, and Xiaoyu Hu^{1,2,3*}**

5 ¹Institute for Immunology and School of Medicine, Tsinghua University, Beijing 100084, China

6 ²Tsinghua-Peking Centre for Life Sciences, Beijing 100084, China

7 ³Beijing Key Laboratory for Immunological Research on Chronic Diseases, Beijing 100084,
8 China

9 ⁴Division of Infectious Diseases, Allergy and Immunology, Department of Internal Medicine,
10 Saint Louis University School of Medicine, Saint Louis University, St. Louis, MO, 63104, USA

11 *Correspondence should be addressed to X. H. (xiaoyuhu@tsinghua.edu.cn).

12

Abstract

Macrophages are critically involved in not only immune and inflammatory responses but also in maintenance of metabolic fitness of organisms. Combined genetic deficiency of three clusters in the miR-17~92 family drastically shifted macrophage phenotypes towards the inflammatory spectrum characterized by heightened production of pro-inflammatory mediator TNF and diminished expression of anti-inflammatory cytokine IL-10. Consequently, macrophages residing in the adipose tissues from myeloid-specific miRNA triple knockout mice spontaneously developed inflammatory phenotypes and displayed alterations of overall physiological conditions as evidenced by obesity and compromised glucose tolerance. Mechanistically, miR-17~92 family miRNAs sustained IL-10 production by promoting transcription of the *Fos* gene, which is secondary to downregulation of *Fos* by transcription factor YY1, a direct target of miR-17~92 family miRNAs. Together, these results identified miR-17~92 family miRNAs as crucial regulators of the balance between pro- and anti-inflammatory cytokines and exemplified how macrophage-intrinsic regulatory circuit exerted impactful influence on general physiology.

Introduction

MicroRNAs are a class of short non-coding RNAs that regulate gene expression post-transcriptionally in metazoan organisms. miRNAs are processed from their primary transcripts (pri-miRNAs) that are cleaved by enzymes Drosha and DiGeorge syndrome critical region gene 8 (DGCR8) into ~70 nucleotide precursors (pre-miRNAs) that are further processed by Dicer into the ~22 nucleotide long mature miRNAs (*Krol et al., 2010*). For approximately 25-40 % of miRNAs, their precursors are located in close proximity to other neighboring precursors on chromatin to form miRNA clusters (*Altuvia et al., 2005; Kozomara and Griffiths-Jones, 2014*), which typically yield mature miRNAs with distinct seed regions that may act coordinately to achieve common functions. miR-17~92 family miRNAs consist of three paralogous miRNA clusters (*Mirc1* (called 'miR-17~92' here) *Mirc2* (called 'miR-106a~363' here) *Mirc3* (called 'miR-106b~25' here)) that encode in total 13 distinct mature miRNAs, which can be further divided into four subfamilies (miR-17, miR-18, miR-19 and miR-25 subfamilies) according to their seed regions (Figure 1-figure supplement 1A and B) (*Mendell, 2008; Ventura et al., 2008*). Genetic studies have shown that global deficiency of the miR-17~92 cluster results in embryonic lethality, whereas deletion of miR-106a~363 or miR-25~363 cluster yields no apparent phenotypes (*Ventura et al., 2008*). Functionally, miR-17~92 family miRNAs play an important role in developmental processes and are regarded as oncogenes during tumorigenesis (*Mendell, 2008; Mogilyansky and Rigoutsos, 2013*). In the immune system, miR-17~92 family miRNAs have been implicated in maintenance of lymphocyte homeostasis, regulation of T follicular helper cell differentiation and modulation of B cell development (*Kang et al., 2013; Lai et al., 2016; Xiao et al., 2008*). However, relatively little is known about the functions of miR-17~92 family miRNAs in myeloid cells including macrophages.

Macrophages play an essential role in maintenance of tissue homeostasis and in innate immunity. In response to various environmental cues, tissue resident macrophages display a wide spectrum of phenotypes ranging from highly inflammatory

ones typically observed upon infections to homeostatic ones during the processes of tissue repair. The spectrum of phenotypes could be partially attributed to the relative quantities of pro- versus anti-inflammatory mediators such as the antagonizing TNF-IL-10 pair (Mosser and Edwards, 2008; Sugimoto et al., 2019). The production of these pro- and anti-inflammatory cytokines is tightly controlled to achieve an intricate balance, and disruption of such balance has been causally linked with pathogenesis of an array of inflammatory and autoimmune diseases such as inflammatory bowel disease (IBD) (Bain and Mowat, 2014). Moreover, the impact of these immune factors reaches far beyond the immune system evidenced by their effects on overall physiological and metabolic conditions. For example, during the development of obesity, pro-inflammatory cytokines such as TNF promote insulin resistance in adipose tissue (Chawla et al., 2011; Olefsky and Glass, 2010). In the obese adipose tissues, macrophages are the most abundant infiltrating immune cells and the major source of pro-inflammatory cytokines (Chawla et al., 2011; Odegaard and Chawla, 2011). Thus, the proper macrophage phenotypes in the adipose tissue microenvironment is critical for maintaining metabolic homeostasis.

In this study, we demonstrated that miR-17~92 family miRNAs critically controlled the balance between pro-inflammatory and anti-inflammatory phenotypes in adipose tissue macrophages. Myeloid specific deletion of three clusters of miR-17~92 family miRNAs twisted adipose tissue macrophages towards a spontaneously inflammatory phenotype characterized by diminished IL-10 and elevated TNF, leading to disrupted adipose homeostasis evidenced by obesity and compromised glucose tolerance. Mechanistically, miR-17~92 family miRNAs prevented inflammation by promoting IL-10 expression through a YY1-Fos-IL-10 regulatory circuit engaging both transcriptional and post-transcriptional mechanisms. Collectively, our results uncovered crucial roles of miR-17~92 family miRNAs in regulating macrophage inflammatory phenotypes in the context of adipose homeostasis.

Results

miR-17~92 family miRNAs protect mice from obesity.

To investigate the function of miR-17~92 family miRNAs, we generated *Mirc2*^{-/-} (called ‘miR-106a~363^{-/-}’ here) *Mirc3*^{-/-} (called ‘miR-106b~25^{-/-}’ here) *Mirc1*^{fllox/fllox} (called ‘miR-17~92^{fllox/fllox}’ here) *Lyz2*-Cre triple knockout (TKO) mice, which efficiently deleted all miRNAs in miR-17~92 family (Figure 1-figure supplement 2A-C). Interestingly, we found that TKO mice consistently exhibited increased body weights than age- and gender-matched *Lyz2*-Cre (WT) control mice at the age of 30 weeks (Figure 1A and Figure 1-figure supplement 3A-C). Then we isolated the visceral adipose tissue (VAT) and brown adipose tissue (BAT) from these mice and found that both the absolute weights of VAT and BAT and the percentages of VAT in TKO mice were significantly higher than those in WT mice (Figure 1B and C and Figure 1-figure supplement 3D). Furthermore, we scanned these mice with magnetic resonance imaging (MRI) and found that the total adipose tissue weight and its percentage of body weight were significantly increased in TKO mice (Figure 1D and E). Thus, these results indicated that miR-17~92 family miRNAs protected mice from obesity. To mimic this chronic obese phenotype, we fed TKO and WT mice with a high-fat diet. Consistent with the results obtained with animals under regular diet, body weights, VAT weights and the VAT percentages of TKO mice were significantly higher than those of WT mice upon 20 weeks of feeding with high fat-diet (Figure 1F-H). Meanwhile, TKO and WT mice were scanned with MRI and MRI quantitation indicated that both total adipose tissue weight and its percentage were significantly increased in TKO mice (Figure 1I and J). To further clarify the physiological role of miR-17~92 family miRNAs in ameliorating obesity, we generated mice deficient of miR-17~92 family miRNAs in the hematopoietic compartment by transferring bone marrow cells from WT and TKO mice into irradiated C57BL/6J or CD45.1 recipients (Figure 1-figure supplement 3E), and subsequently fed these chimeric mice with a regular chow diet or high-fat diet. TKO chimeric mice also exhibited increased body weights compared with WT chimeric mice (Figure 1K and Figure 1-figure supplement 3F). Moreover, the absolute weights and the percentages of VAT and total adipose tissue were significantly increased in TKO chimeric mice (Figure 1L-O). In summary, these results demonstrate that myeloid-

intrinsic miR-17~92 family miRNAs protect mice from obesity.

miR-17~92 family miRNAs maintain adipose tissue macrophage homeostasis.

We next thought to investigate the mechanisms by which miR-17~92 family miRNAs protected mice from obesity. As obesity is often associated with insulin resistance, we firstly examined the glucose homeostasis in TKO and WT mice with glucose tolerance test (GTT) and found that TKO mice showed higher insulin resistance than control animals (Figure 2A). It is well established that pro-inflammatory cytokine TNF and anti-inflammatory cytokine IL-10 are critical in regulating the insulin sensitivity and obesity (*Chawla et al., 2011; Olefsky and Glass, 2010*), we firstly detected TNF and IL-10 levels in serum of WT and TKO mice and found increased TNF and decreased IL-10 proteins in TKO mice relative to WT animals (Figure 2-figure supplement 1A and B). Then we examined the expression of *Tnf* and *Il10* mRNA in WT and TKO VAT by quantitative real-time PCR (qPCR). We found that the expression of *Tnf* was significantly higher whereas the expression of *Il10* was significantly lower in TKO VAT than those in WT VAT (Figure 2B and Figure 2-figure supplement 1C and D). As macrophages are reported to be the major immune cells producing these cytokines in the VAT (*Chawla et al., 2011; Odegaard and Chawla, 2011*), we firstly analyzed the adipose tissue macrophage (ATM) population in VAT of WT and TKO mice. miR-17~92 family miRNAs were efficiently deleted in TKO ATMs (Figure 2-figure supplement 2A-E) and their deficiency did not alter the population of ATMs in mice (Figure 2C and D and Figure 2-figure supplement 3A-E). Furthermore, genome wide RNA profiling analyses were performed with fluorescence-activated cell sorting (FACS) sorted ATMs from WT and TKO mice fed with regular chow diet or high fat diet. Gene ontology (GO) analysis indicated that genes differentially expressed in both TKO verses WT mice and high fat diet verses chow diet fed WT mice were enriched in the inflammatory response category (Figure 2E and Figure 2-figure supplement 4A). Meanwhile, the inflammatory score indexing cellular inflammatory phenotypes calculated based on the RNA sequencing data indicated that ATMs from TKO mice were more inflammatory than the WT counterparts under both regular chow diet and

high fat diet conditions (Figure 2-figure supplement 4B). Moreover, both RNA sequencing results and qPCR results showed that TKO ATMs expressed increased *Tnf* and decreased *Il10* (Figure 2F-H and Figure 2-figure supplement 4C and D). Thus, these results demonstrated that miR-17~92 family miRNA deficiency shifts adipose tissue macrophage towards an inflammatory phenotype characterized by TNF overproduction in the absence of exogenous infectious or inflammatory signals, suggesting that miR-17~92 family miRNAs maintain adipose tissue macrophage homeostasis to prevent obesity and to facilitate glucose tolerance.

miR-17~92 family miRNAs balance TNF and IL-10 production in macrophages.

To circumvent the technical limitation imposed by relatively scarce number of ATMs, we next utilized bone marrow-derived macrophages (BMDMs) for further mechanistic studies. Compared to WT controls, basal expression of *Tnf* mRNA and of *Il10* mRNA was consistently up-regulated and down-regulated respectively in TKO BMDMs (Figure 3A and B and Figure 3-figure supplement 1A and B), recapitulating the above observations in ATMs. Notably, due to heightened expression of these cytokine genes in TLR-activated especially LPS-stimulated conditions, upregulation or downregulation of *Tnf* and *Il10* expression became more appreciable in activated macrophages than in resting cells (Figure 3C and D and Figure 3-figure supplement 1C-F). The mRNA expression patterns were further corroborated with alterations of TNF and IL-10 protein production by TKO macrophages (Figure 3E and F). Next, in order to clarify the connection between TNF and IL-10 in TKO BMDMs, we supplemented recombinant IL-10 protein prior to LPS stimulation and found that with sufficient quantity of IL-10, TNF production by TKO BMDMs reduced to a comparable level as WT BMDMs (Figure 3G). Moreover, blockade of IL-10 receptor with an anti-IL-10R antibody prior to LPS stimulation diminished the differences of TNF production observed between WT and TKO BMDMs (Figure 3-figure supplement 1G), implying that overexpression of TNF was likely secondary to inadequate amount of IL-10 produced by TKO cells. To functionally correct the obese phenotypes of TKO mice, an anti-TNF antibody or PBS was administrated weekly to TKO and WT mice along with

high fat diet for 20 weeks. The anti-TNF treatment significantly reversed the obese phenotypes of TKO mice (Figure 3H), indicating that TNF was a functional target of miR-17~92 family miRNAs in regulating obesity. Overall, these results suggested that miR-17~92 family miRNAs suppressed TNF-mediated inflammation through promoting IL-10 expression in macrophages.

As miR-17~92 family miRNAs consist of three distinct clusters (Figure 1-figure supplement 1A and B), next we examined the relative contribution of each miRNA cluster in regulating TNF and IL-10 expression. Deletion of individual cluster or double deficiency of miR-106a~363 and miR-106b~25 clusters (DKO) did not significantly alter LPS-induced *Tnf* expression in macrophages (Figure 4A-D). Expression of *Il10* showed modest reduction in individual cluster single KO as well as in DKO BMDMs (Figure 4E-H). To investigate the collective effects of these three clusters, we compared fold changes of *Tnf* and *Il10* expression over their respective WT controls among macrophages harboring various genotypes of miRNA deficiency and found that *Tnf* was only markedly upregulated upon deletion of all three clusters while the extent of *Il10* down-regulation largely correlated with the number of deleted miRNA clusters (Figure 4I and J). Taken together, these results indicated that three miRNA clusters of miR-17~92 family collectively inhibited TNF and promoted IL-10 expression in macrophages.

miR-17~92 family miRNAs promote IL-10 production via sustaining *Fos* expression.

Having established IL-10 as a key target of miR-17~92 family miRNAs-mediated regulation in macrophages, we then sought to identify the mechanisms by which they promote IL-10 expression. As PTEN is a well-studied target of miR-17~92 family miRNAs (O'Donnell *et al.*, 2005; Xiao *et al.*, 2008) and PTEN and its related molecules have been implicated in modulating IL-10 expression (Hu *et al.*, 2006; Martin *et al.*, 2005), we firstly investigated whether miR-17~92 family miRNAs regulated IL-10 and TNF through targeting PTEN. Inhibition of PTEN phosphatase activity by a chemical

inhibitor in TKO BMDMs did not apparently alter expression of IL-10 and TNF, suggesting that the regulation of TNF and IL-10 by miR-17~92 family miRNAs was independent of PTEN (Figure 5-figure supplement 1A and B). To further explore how IL-10 was regulated by miR-17~92 family miRNAs, we performed genome-wide expression profiling analysis in TKO and WT BMDMs (Zhang *et al.*, 2020). Interestingly, we found that *Fos*, encoding a key component of transcriptional factor AP-1 that drives the expression of IL-10 (Hu *et al.*, 2006; Saraiva and O'Garra, 2010), was down-regulated in TKO BMDMs compared to WT controls whereas the expression of other reported targets of miR-17~92 family miRNAs remained minimally affected (Figure 5A). Then we experimentally confirmed that *Fos* was consistently and significantly decreased in TKO BMDMs at both mRNA and protein levels (Figure 5B-E and Figure 5-figure supplement 2A and B). In contrast to *Fos*, the expression of *Jun*, another key component of AP-1 complex, did not apparently differ between WT and TKO BMDMs (Figure 5-figure supplement 3A and B). Furthermore, overexpression of *Fos* in TKO BMDMs rescued the reduced expression of IL-10 and the enhanced expression of TNF to the levels comparable with that in WT cells (Figure 5 F-H and Figure 5-figure supplement 4A and B), indicating that subdued expression of IL-10 in TKO BMDMs was likely resulted from diminished *Fos* activities. Thus, these data demonstrated that miR-17~92 family miRNAs promoted IL-10 production via sustaining the expression of *Fos*.

miR-17~92 family miRNAs directly target YY1 to regulate *Fos* expression.

Having demonstrated that miR-17~92 family miRNAs regulate IL-10 by sustaining the expression of *Fos*, we next sought to investigate how *Fos* was regulated by miR-17~92 family miRNAs. In previous studies, *Fos* is reported to be inhibited by a transcriptional factor YY1 (Shi *et al.*, 1997). Interestingly, despite the fact that the mRNA levels of *Yy1* were comparable between WT and TKO BMDMs, YY1 protein was significantly increased in TKO BMDMs (Figure 6A-C), implying post-transcriptional regulation of YY1 by miR-17~92 family miRNAs. Bioinformatics analysis with the miRanda tool (Betel *et al.*, 2010) revealed YY1 as a predicted target of the miR-17 family miRNAs,

a subfamily of miR-17~92 family miRNAs (Figure 6D). Luciferase reporter assays with the constructs containing *Yy1* 3'UTR showed significant attenuation of luciferase activities by miRNAs from miR-17~92, miR-106a~363, or miR-106b~25 cluster, whereas mutation of the miR-17 family miRNAs' binding sites on *Yy1* 3'UTR reversed such inhibitory effects (Figure 6E), suggesting that YY1 was likely to be the direct target of miR-17~92 family miRNAs. To further validate the involvement of YY1 in miR-17~92 family miRNAs-mediated regulation of Fos, we knocked down YY1 expression by RNA interference in WT and TKO BMDMs (Figure 6-figure supplement 1A-C). Knocking down YY1 significantly up-regulated the expression of Fos at the mRNA and protein levels (Figure 6F-H and Figure 6-figure supplement 2A and B) and subsequently decreased TNF and increased IL-10 expression (Figure 6I-L). Collectively, these results suggested that miR-17~92 family miRNAs promoted Fos expression by releasing YY1-mediated inhibition.

Discussion

In the immune system, miR-17~92 family miRNAs have been predominantly studied in adaptive immune cells including T cells and B cells. However, the functions of miR-17~92 family miRNAs in innate immune cells remain elusive. Here, we illustrated the previously unidentified functions as well as underlying mechanisms of miR-17~92 family miRNAs in regulating the balance between key pro- and anti-inflammatory mediators in macrophages and uncovered a novel target of miR-17~92 family miRNAs (Figure 6-figure supplement 3). Such regulation bears important biological outcomes in the context of macrophage-mediated chronic inflammation with impact on general physiology such as body weight and glucose tolerance.

In recent years, due to life style changes such as increased intake of refined foods, the incidence of obesity has risen dramatically all over the globe, which in turn leads to an explosion of obesity-related disorders including but not limited to insulin resistance and type 2 diabetes, fatty liver disease and cardiovascular diseases (*Finucane et al., 2011; González-Muniesa et al., 2017*). A variety of factors have been implicated in

development of obesity, including dysregulation of interconnected endocrine circuits, systemic chronic inflammation and certain cell-intrinsic mechanisms such as oxidative stress, mitochondrial dysfunction and endoplasmic reticulum (ER) stress (*Hotamisligil, 2006; Jaitin et al., 2019; Kahn and Flier, 2000; Qatanani and Lazar, 2007*). Immune modulating cytokines including TNF and IL-10 are also critical regulators of insulin signaling (*Chawla et al., 2011; Olefsky and Glass, 2010*). For example, TNF activated signaling molecules such as IKK, JNK, S6 kinase and mammalian target of rapamycin (mTOR) could potentially phosphorylate insulin receptor substrate 1 (IRS1) to attenuate insulin signaling and subsequently contribute to development of insulin resistance (*Gao et al., 2002; Gao et al., 2003; Hirosumi et al., 2002; Lee et al., 2007; Ozes et al., 2001; Yin et al., 1998*). Although miR-17~92 family miRNAs have been reported to regulate adipocyte development (*Chen et al., 2014; Wang et al., 2008*), the current study depicted a miR-17~92 family miRNA-centric immune circuit operative in macrophages that indirectly controls metabolic phenotypes such as insulin resistance and obesity.

Previous studies have implicated roles of miR-17~92 family miRNAs in developmental processes and tumorigenesis (*Mendell, 2008; Mogilyansky and Rigoutsos, 2013*), and validated multiple targets including E2F1 (*O'Donnell et al., 2005*), PTEN (*O'Donnell et al., 2005; Xiao et al., 2008*), Bim (*Ventura et al., 2008; Xiao et al., 2008*), PHLPP2 (*Kang et al., 2013*) and C/EBP β (*Kang et al., 2020*). In this study we identified YY1 as a novel target of miR-17~92 family miRNAs. Attenuation of YY1 protein by macrophage-intrinsic miR-17~92 family miRNAs sustains expression of Fos and thus activities of a key transcription complex AP-1, resulting in optimal expression of a major homeostatic cytokine IL-10 and restraining cells from overactivation. To our knowledge, these results represent the first experimental evidence for suggesting an immune-regulatory role of YY1 in myeloid cells. The detailed analyses of regulation and function of transcription factor YY1 in macrophages warrants future investigation. Nevertheless, despite of identification of YY1 as a target of miR-17~92 family miRNAs, we cannot exclude the possibility that other miRNA

targets may be involved in regulating macrophage phenotypes. Further studies are needed to fully elucidate the mechanisms by which miR-17~92 family miRNAs regulate macrophage biology.

TNF is a pro-inflammatory cytokine critical for host defense against bacterial, viral and parasitic infections, yet excessive production of TNF has been causally linked with multiple autoimmune and inflammatory diseases such as rheumatoid arthritis, inflammatory bowel disease and diabetes (Bradley, 2008; Brenner *et al.*, 2015). Thus, the production of TNF must be tightly controlled by a variety of negative regulators. IL-10 is a potent anti-inflammatory cytokine that plays a central role in resolution of inflammation and robustly suppresses production of inflammatory mediators such as TNF via transcriptional and post-transcriptional mechanisms (Moore *et al.*, 2001; Ouyang and O'Garra, 2019). Full-fledged expression of IL-10 by macrophages is achieved by coordinated action of transcription factors including c-Maf and AP-1 (Cao *et al.*, 2005; Ouyang *et al.*, 2011; Saraiva and O'Garra, 2010). Here we identified miR-17~92 family miRNAs as key positive regulators supporting IL-10 production in ATMs, raising possibilities for this family of miRNAs as potential therapeutic targets of inflammatory and metabolic disorders.

Materials and Methods

Key Resources Table				
Reagent type (species) or resource	Designation	Source or reference	Identifiers	Additional information
Genetic reagent (<i>Mus. musculus</i>)	<i>Lyz2-Cre</i>	The Jackson Laboratory	Stock No: 004781	

Genetic reagent (<i>Mus. musculus</i>)	C57BL/6J	The Jackson Laboratory	Stock No: 000664	
Genetic reagent (<i>Mus. musculus</i>)	miR-106a~363 ^{-/-} (<i>Mirc2^{-/-}</i>)	The Jackson Laboratory	Stock No: 008461	
Genetic reagent (<i>Mus. musculus</i>)	miR-106b~25 ^{-/-} (<i>Mirc3^{-/-}</i>)	The Jackson Laboratory	Stock No: 008460	
Genetic reagent (<i>Mus. musculus</i>)	miR-17~92 ^{flox/flox} (<i>Mirc1^{flox/flox}</i>)	The Jackson Laboratory	Stock No: 008458	
Genetic reagent (<i>Mus. musculus</i>)	miR-106a~363 ^{-/-} miR-106b~25 ^{-/-} (<i>Mirc2^{-/-} Mirc3^{-/-}</i>)	This paper	N/A	
Genetic reagent (<i>Mus. musculus</i>)	miR-106a~363 ^{-/-} miR-106b~25 ^{-/-} miR-17~92 ^{flox/flox} <i>Lyz2-Cre (Mirc2^{-/-} Mirc3^{-/-} Mirc1^{flox/flox} Lyz2-Cre)</i>	This paper	N/A	
Genetic reagent (<i>Mus. musculus</i>)	CD45.1	Gift from Dr. Yan Shi, Tsinghua University	N/A	
Genetic reagent (<i>Mus. musculus</i>)	<i>Lyz2-RFP</i>	Gift from Dr. Yuncai Liu, Tsinghua University	N/A	

cell line (<i>Homo. sapiens</i>)	293T	ATCC	ACS-4500	
antibody	Anti-mouse F4/80-APC (Rat monoclonal)	eBioscience	Cat# 17-4801-82, RRID:AB_2784648	1:400
antibody	Anti-mouse CD45-APC/Cy7 (Rat monoclonal)	BioLegend	Cat# 103116, RRID:AB_312981	1:400
antibody	Anti-mouse CD11b-PerCP-Cy5.5 (Rat monoclonal)	eBioscience	Cat# 45-0112-82, RRID:AB_953558	1:400
antibody	Anti-mouse Mer-BV605 (Rat monoclonal)	BD Biosciences	Cat# 747894	1:400
antibody	Anti-mouse CD64-PE (Mouse monoclonal)	BioLegend	Cat# 139304, RRID:AB_10612740	1:200
antibody	Anti-mouse CD11c-FITC (Hamster monoclonal)	BD Biosciences	Cat# 553801, RRID:AB_395060	1:400
antibody	Anti-mouse CX ₃ CR1-PE/Cy7 (Mouse monoclonal)	BioLegend	Cat# 149015, RRID:AB_2565699	1:400
antibody	Anti-mouse Ly6C-Alexa Fluor 700 (Rat monoclonal)	BioLegend	Cat# 128024, RRID:AB_10643270	1:400

antibody	Anti-mouse CD45.1-BV421(Mouse monoclonal)	BioLegend	Cat# 110732, RRID:AB_2562563	1:400
antibody	Anti-mouse CD45.2-PE/Cy7 (Mouse monoclonal)	eBioscience	Cat# 25-0454-80, RRID:AB_2573349	1:400
antibody	p38 α (C-20) (Rabbit polyclonal)	Santa Cruz Biotechnology	Cat# sc-535, RRID:AB_632138	1:1000
antibody	c-Fos Antibody (4) (Rabbit polyclonal)	Santa Cruz Biotechnology	Cat# sc-52, RRID:AB_2106783	1:1000
antibody	c-Jun (60A8) (Rabbit monoclonal)	Cell Signaling Technology	Cat# 9165, RRID:AB_2130165	1:1000
antibody	YY1 antibody [EPR4652] (Rabbit monoclonal)	Abcam	Cat# ab109237, RRID:AB_10890662	1:1000
antibody	Anti-mouse IL-10R (Rat monoclonal)	Bio X Cell	Cat# BE0050, RRID:AB_1107611	
antibody	rat IgG1 isotype control (Rat monoclonal)	Bio X Cell	Cat# BE0088, RRID:AB_1107775	
antibody	Anti-mouse TNF α (Rat monoclonal)	Bio X Cell	Cat# BP0058, RRID:AB_1107764	

recombinant DNA reagent	psiCHECK-2-YY1-WT (Plasmid)	This paper	N/A	
recombinant DNA reagent	psiCHECK-2-YY1-Mut (Plasmid)	This paper	N/A	
sequenced-based reagent	YY1 siRNA	GenePharma	N/A	GAAC UCAC CUCC UGAU UAU (sense), AUA UCAG GAGG UGAG UUC (antisense)
sequenced-based reagent	Primers for qPCR	This Paper	N/A	see Supplementary file 1
peptide, recombinant protein	Recombinant Murine IL-10	PeproTech	Cat# 210-10	
commercial assay or kit	Total RNA Miniprep Purification Kit	GeneMark	TR01-150	
commercial assay or kit	Mouse TNF ELISA Set	BD Biosciences	Cat# 555268	
commercial assay or kit	IL-10 ELISA Kit	BioLegend	Cat# 431414	
commercial assay or kit	TaqMan microRNA	Applied Biosystems	Cat# 4366596	

	Reverse Transcription Kit			
commercial assay or kit	TaqMan MicroRNA assays	Applied Biosystems	Cat# 4427975	
commercial assay or kit	Dual-Luciferase® Reporter Assay System	Promega	Cat# E1910	
chemical compound, drug	SF1670	Selleck	Cat# S7310	
chemical compound, drug	LPS-EB (LPS from E. coli O111:B4)	InvivoGen	Cat# tlr-ebmps	
chemical compound, drug	Pam3CSK4	InvivoGen	Cat# tlr-pms	
chemical compound, drug	Lipofectamine™ 2000 Transfection Reagent	Invitrogen	Cat# 11668027	
chemical compound, drug	TransIT-TKO® Transfection Reagent	Mirus	Cat# MIR2150	
software, algorithm	GraphPad Prism	GraphPad Software	RRID:SCR_002798	
software, algorithm	FlowJo(v10.0.7)	FlowJo	RRID:SCR_008520	
software, algorithm	Image J (v1.52a)	https://imagej.nih.gov/ij/index.html	RRID:SCR_003070	

Mice. The miR-106a~363^{-/-} (*Mirc2*^{-/-}, Jax stock #008461), miR-106b~25^{-/-} (*Mirc3*^{-/-}, Jax stock #008460), and miR-17~92^{flox/flox} (*Mirc1*^{flox/flox}, Jax stock #008458) mice were purchased from The Jackson Laboratory, which were all on C57BL/6J background. miR-17~92^{flox/flox} were crossed with *Lyz2*-Cre mice to obtain mice with myeloid specific deletion of miR-17~92 cluster. The miR-106a~363 and miR-106b~25 miRNA clusters double KO mice were obtained by crossing miR-106a~363^{-/-} mice with miR-106b~25^{-/-} mice. The miR-17~92, miR-106a~363, and miR-106b~25 clusters triple KO mice were obtained by crossing miR-106a~363^{-/-} miR-106b~25^{-/-} mice with miR-17~92^{flox/flox} *Lyz2*-Cre mice. CD45.1 mice were kindly provided by Dr. Yan Shi (Tsinghua University). *Lyz2*-RFP mice were kindly provided by Dr. Yuncai Liu (Tsinghua University) which were originally bred from *Lyz2*-Cre and ROSA-tdRFP mice (Luche *et al.*, 2007). Experiments were performed with mice at 6-8 weeks of age unless otherwise specified with age and gender matched controls. Wild-type C57BL/6J mice were used as controls for miR-106a~363^{-/-}, miR-106b~25^{-/-}, and miR-106a~363^{-/-} miR-106b~25^{-/-} mice, and *Lyz2*-Cre mice were used as controls for miR-17~92^{flox/flox} *Lyz2*-Cre and miR-106a~363^{-/-} miR-106b~25^{-/-} miR-17~92^{flox/flox} *Lyz2*-Cre mice. All experiments using mice were approved by the Institutional Animal Care and Use Committees at Tsinghua University (Protocol #17-HXY1).

Cell culture and reagents. Murine BMDMs were obtained as previously described (Xu *et al.*, 2012) and maintained in DMEM (HyClone) supplemented with 10% FBS (Gibco) and 10% supernatant of L929 cell as conditioned medium providing macrophage colony-stimulating factor (M-CSF, identified as complete medium). Briefly, bone marrow cells were extracted and cultured with complete medium for 5 days to derive BMDMs. Cell culture grade LPS and Pam3CSK4 was purchased from Invivogen and were used at concentration of 10 ng/ml unless otherwise specified. SF1670 were from Selleck. anti-IL10R, anti-IgG and anti-TNF were purchased from BioXCell. anti-IL10R or anti-IgG were added 30 min prior to LPS stimulation and were present throughout LPS exposure.

350

351 **Reverse transcription and qPCR.** RNA was extracted from whole cell lysates and
352 was reversely transcribed to cDNA as previously described (*Zhang et al., 2019*). qPCR
353 was performed with an ABI StepOnePlus thermal cycler. Primary transcripts were
354 measured with primers that amplify either exon-intron junctions or intronic sequences.
355 Threshold cycle numbers were normalized to samples amplified with primers specific
356 for glyceraldehyde-3-phosphate dehydrogenase (*Gapdh*). For qPCR analysis of mature
357 miRNA, cDNA was prepared from total RNA, which was isolated with TRIzol reagent
358 (Invitrogen), with the TaqMan microRNA Reverse Transcription Kit (Applied
359 Biosystems). TaqMan MicroRNA assays were used according to the manufacturer's
360 recommendations (Applied Biosystems) for real-time PCR. Expression of U6 snRNA
361 was used for normalization of expression values. Primer sequences are listed in the
362 Supplementary file 1.

363

364 **Enzyme-linked immunosorbent assay (ELISA).** Cytokine secretion was quantified
365 with TNF (BD Biosciences) or IL-10 (Biolegend) ELISA kit according to the
366 manufacturers' instructions.

367

368 **Bone marrow chimeras.** Bone marrow chimeras were generated as previously
369 described (*Hu et al., 2008*). Briefly, 6-week-age recipient C57BL/6J mice or CD45.1
370 mice were irradiated twice at a dose of 5.5 Gy with 3 hours break in between, followed
371 by intravenous injection of 10^6 donor bone marrow cells from WT or TKO mice.
372 Chimeric mice were used for experiments 6 weeks after the initial bone marrow transfer.

373

374 **High-fat diet induced obesity.** Mice were fed with a high-fat diet and body weight
375 was measured weekly for 13-28 weeks. Mice were scanned with magnetic resonance
376 imaging (MRI) machine (QMR06-090H, NIUMAG) for analysis of body composition

before scarification for visceral adipose tissue excision. Visceral adipose tissue weight was measured and was calculated for the percentage of body weight.

Glucose tolerance test. Mice were injected intraperitoneally with glucose (2 mg/g of body weight) after fasting overnight (14-16 h). The levels of blood glucose were measured with a glucometer (GA-3, SANNUO).

Isolation of cells from adipose tissue. Mice were sacrificed and visceral adipose tissue were removed and cut into small pieces. Then tissues were digested in 5 ml ice cold digestion buffer (RPMI 1640 medium containing 10% FBS, 2 mg/ml Collagenase IV (Sigma-Aldrich) and 50 µg/ml DNaseI (Sigma-Aldrich)) for 45 min at 37 °C with rotation (200 rpm). The digested tissues were passed through a 70 µm cell strainer and centrifugated at 1,500 rpm for 10 min to get the isolated cells.

Flow cytometry. Cells from adipose tissues were prepared and lysed with ACK lysing buffer (Gibco) to exclude red blood cells and were stained with antibodies on ice for 30 min in the dark. APC/Cy7 anti-mouse CD45 (30-F11, BioLegend), Percpcy5.5 anti-mouse CD11b (M1/70, eBioscience), APC anti-mouse F4/80 (BM8, eBioscience) were used to stain adipose tissue macrophages, and BV605 anti-mouse Mer (108928, BD Biosciences), PE anti-mouse CD64 (X54-5/7.1 BioLegend), FITC anti-mouse CD11c (HL3, BD Biosciences), PE/Cy7 anti-mouse CX₃CR1 (SA011F11, BioLegend), Alexa Fluor 700 anti-mouse Ly6C (HK1.4, BioLegend) were used to further analyze surface markers of ATMs, BV421 anti-mouse CD45.1 (A20, BioLegend) and PE/Cy7 anti-mouse CD45.2 (104, eBioscience) were used to identify ATMs from CD45.1 and CD45.2 mice, all antibodies were used in 1:400 dilutions except CD64 (used in 1:200 dilutions). Cells were washed three times and were performed on FACSFortessa or FACS Aria III flow cytometer (BD Biosciences) and analyzed with FlowJo software (Tree Star).

Immunoblotting analysis. Whole cell lysates were prepared as described previously (Xu *et al.*, 2012). For immunoblotting analysis, lysates were separated by 10% SDS-PAGE and transferred to a PVDF membrane (Millipore) for probing with antibodies. The antibodies against p38 (sc-535) and c-Fos (sc-52) were purchased from Santa Cruz Biotechnology, YY1 antibody (ab109237) was purchased from Abcam, c-Jun antibody (#9165) was obtained from Cell Signaling Technology.

RNA sequencing and analysis. Total RNA was isolated with TRIzol reagent (Invitrogen) from whole cell lysates of ATMs from WT and TKO mice fed with regular chow diet or high fat diet (HFD). RNA was isolated, librated, and sequenced with Illumina Novaseq platform by Novogene (Novogene; Beijing, China). Total reads were cleaned and mapped to the mm10 reference genome and then were normalized as fragments per kilobase of transcript per million mapped reads (FPKM). Upregulated and downregulated genes in TKO ATMs were identified as $p\text{-value} \leq 0.05$, (FPKM +1) fold changes (TKO/WT) ≥ 1.6 for upregulated genes and (FPKM +1) fold changes (TKO/WT) ≤ 0.6 for downregulated genes. Differential expressed genes (DEGs) between WT-HFD and WT ATMs were defined as a $p\text{-value} \leq 0.05$ and absolute value of \log_2 ratio (WT-HFD/WT) ≥ 1 . Gene ontology (GO) analysis was conducted with up and down regulated genes in TKO verses WT ATMs group and DEGs in WT-HFD verses WT ATM group by Enrichr (Chen *et al.*, 2013; Kuleshov *et al.*, 2016). Inflammatory score was calculated with the following formula: Inflammatory score = sum of \log (FPKM+1) of representative pro-inflammatory genes (*Tnf*, *Il6*, *Cxcl1*, *Ccl2* and *Ccl8*) - sum of \log (FPKM+1) of representative anti-inflammatory genes (*Il10*, *Il4*, *Il5* and *Il13*). RNA-seq datasets with WT and TKO BMDMs from our previous published work (Zhang *et al.*, 2020) were re-analyzed and plotted.

Luciferase reporter assay. The psiCHECK2 (Promega) reporter plasmid were cloned with 3'-UTR fragments of *Yy1* containing wild-type or mutated predicted binding sites

of miR-17 family miRNAs (Supplementary file 2) to generate *Yy1* reporter plasmids. 293T cells were plated into 24-well plates at 1×10^5 cells per well 24 h before transfection with 10 ng reporter plasmid and 500 ng overexpression vectors encoding miRNAs of miR-17~92, miR-106a~363, or miR-106b~25 clusters using the Lipofectamine 2000 transfection reagent (Invitrogen). Luciferase assays were performed 48 h post transfection using the Dual-Luciferase Reporter Assay System (Promega) following the manufacturer's protocol. The renilla firefly luciferase (Rluc) activity was normalized by the firefly luciferase activity (Luc) and expression is presented as Rluc/Luc ratio.

Cell lines. 293T cells (ATCC ACS-4500) were maintained in DMEM supplemented with 10% FBS and 1% Penicillin-Streptomycin (Gibco) and tested negative for mycoplasma.

RNA-mediated interference. Small interfering RNA (siRNA) specifically targeting mouse *Yy1* (5'-GAACU CACCU CCUGA UUAU-3' (sense)/ 5'-AUAAU CAGGA GGUGA GUUC-3' (antisense)) and nontargeting control siRNA were from GenePharma. The siRNAs were transfected into mouse BMDMs through the use of TransIT TKO transfection reagent according to the manufacturer's instructions (Mirus Bio). Cells were then lysed for mRNA and protein extraction 48 h post transfection.

Statistical Analysis. P values were calculated with a two-tailed paired or unpaired Student's *t*-test or two-way ANOVA. Not significant, $P > 0.05$; * $P < 0.05$; ** $P < 0.01$; *** $P < 0.001$; and **** $P < 0.0001$.

Data and materials availability: All data supporting the findings of this study are presented within the article and its supplementary files, or available from the

corresponding author upon reasonable request. The RNA-seq data set is deposited in the National Center for Biotechnology Information Gene Expression Omnibus under accession number GSE129613 (Zhang *et al.*, 2020) and GSE158627.

Acknowledgements: We thank Y. Zhang (University of Maryland) and B. Zhang (Tsinghua University) for help with RNA-seq analysis and Y. Shi (Tsinghua University) and Y. Liu (Tsinghua University) for kindly providing several mouse strains. This research was supported by National Natural Science Foundation of China grants (31725010 and 31821003 to X.H. and 31330027 to L.W.), funds from Tsinghua-Peking Center for Life Sciences (X.Z., X.H., and L.W.), and funds from Institute for Immunology at Tsinghua University (X.H. and L.W.).

Competing interests: The authors declare no competing financial interests.

References

- Altuvia, Y., Landgraf, P., Lithwick, G., Elefant, N., Pfeffer, S., Aravin, A., Brownstein, M.J., Tuschl, T., and Margalit, H. 2005. Clustering and conservation patterns of human microRNAs. *Nucleic Acids Res* **33**, 2697-2706. doi: 10.1093/nar/gki567
- Bain, C.C., and Mowat, A.M. 2014. Macrophages in intestinal homeostasis and inflammation. *Immunol Rev* **260**, 102-117. doi: 10.1111/imr.12192
- Betel, D., Koppal, A., Agius, P., Sander, C., and Leslie, C. 2010. Comprehensive modeling of microRNA targets predicts functional non-conserved and non-canonical sites. *Genome Biol* **11**, R90. doi: 10.1186/gb-2010-11-8-r90
- Bradley, J.R. 2008. TNF-mediated inflammatory disease. *J Pathol* **214**, 149-160. doi: 10.1002/path.2287
- Brenner, D., Blaser, H., and Mak, T.W. 2015. Regulation of tumour necrosis factor signalling: live or let die. *Nat Rev Immunol* **15**, 362-374. doi: 10.1038/nri3834
- Cao, S., Liu, J., Song, L., and Ma, X. 2005. The Protooncogene c-Maf Is an Essential Transcription Factor for IL-10 Gene Expression in Macrophages. *The Journal of*

489 *Immunology* **174**, 3484-3492. doi: 10.4049/jimmunol.174.6.3484

490 Chawla, A., Nguyen, K.D., and Goh, Y.P. 2011. Macrophage-mediated inflammation in
491 metabolic disease. *Nat Rev Immunol* **11**, 738-749. doi: 10.1038/nri3071

492 Chen, E.Y., Tan, C.M., Kou, Y., Duan, Q., Wang, Z., Meirelles, G.V., Clark, N.R., and
493 Ma'ayan, A. 2013. Enrichr: interactive and collaborative HTML5 gene list enrichment
494 analysis tool. *BMC Bioinformatics* **14**, 128. doi: 10.1186/1471-2105-14-128

495 Chen, L., Cui, J., Hou, J., Long, J., Li, C., and Liu, L. 2014. A Novel Negative Regulator
496 of Adipogenesis: MicroRNA-363. *Stem Cells* **32**, 510-520. doi: 10.1002/stem.1549

497 Finucane, M.M., Stevens, G.A., Cowan, M.J., Danaei, G., Lin, J.K., Paciorek, C.J.,
498 Singh, G.M., Gutierrez, H.R., Lu, Y., Bahalim, A.N., Farzadfar, F., Riley, L.M., and
499 Ezzati, M. 2011. National, regional, and global trends in body-mass index since 1980:
500 systematic analysis of health examination surveys and epidemiological studies with 960
501 country-years and 9·1 million participants. *The Lancet* **377**, 557-567. doi:
502 [https://doi.org/10.1016/S0140-6736\(10\)62037-5](https://doi.org/10.1016/S0140-6736(10)62037-5)

503 Gao, Z., Hwang, D., Bataille, F., Lefevre, M., York, D., Quon, M.J., and Ye, J. 2002.
504 Serine Phosphorylation of Insulin Receptor Substrate 1 by Inhibitor κ B Kinase
505 Complex. *J Biol Chem* **277**, 48115-48121. doi: 10.1074/jbc.M209459200

506 Gao, Z., Zuberi, A., Quon, M.J., Dong, Z., and Ye, J. 2003. Aspirin Inhibits Serine
507 Phosphorylation of Insulin Receptor Substrate 1 in Tumor Necrosis Factor-treated Cells
508 through Targeting Multiple Serine Kinases. *J Biol Chem* **278**, 24944-24950. doi:
509 10.1074/jbc.M300423200

510 González-Muniesa, P., Martínez-González, M.-A., Hu, F.B., Després, J.-P., Matsuzawa,
511 Y., Loos, R.J.F., Moreno, L.A., Bray, G.A., and Martinez, J.A. 2017. Obesity. *Nat Rev*
512 *Dis Primers* **3**, 17034. doi: 10.1038/nrdp.2017.34

513 Hirosumi, J., Tuncman, G., Chang, L., Görgün, C.Z., Uysal, K.T., Maeda, K., Karin,
514 M., and Hotamisligil, G.S. 2002. A central role for JNK in obesity and insulin resistance.
515 *Nature* **420**, 333-336. doi: 10.1038/nature01137

516 Hotamisligil, G.S. 2006. Inflammation and metabolic disorders. *Nature* **444**, 860-867.
517 doi: 10.1038/nature05485

518 Hu, X., Chung, A.Y., Wu, I., Foldi, J., Chen, J., Ji, J.D., Tateya, T., Kang, Y.J., Han, J.,

Gessler, M., Kageyama, R., and Ivashkiv, L.B. 2008. Integrated Regulation of Toll-like Receptor Responses by Notch and Interferon- γ Pathways. *Immunity* **29**, 691-703. doi: <https://doi.org/10.1016/j.immuni.2008.08.016>

Hu, X., Paik, P.K., Chen, J., Yarilina, A., Kockeritz, L., Lu, T.T., Woodgett, J.R., and Ivashkiv, L.B. 2006. IFN-gamma suppresses IL-10 production and synergizes with TLR2 by regulating GSK3 and CREB/AP-1 proteins. *Immunity* **24**, 563-574. doi: 10.1016/j.immuni.2006.02.014

Jaitin, D.A., Adlung, L., Thaïss, C.A., Weiner, A., Li, B., Descamps, H., Lundgren, P., Bleriot, C., Liu, Z., Deczkowska, A., Keren-Shaul, H., David, E., Zmora, N., Eldar, S.M., Lubezky, N., Shibolet, O., Hill, D.A., Lazar, M.A., Colonna, M., Ginhoux, F., Shapiro, H., Elinav, E., and Amit, I. 2019. Lipid-Associated Macrophages Control Metabolic Homeostasis in a Trem2-Dependent Manner. *Cell* **178**, 686-698.e614. doi: <https://doi.org/10.1016/j.cell.2019.05.054>

Kahn, B.B., and Flier, J.S. 2000. Obesity and insulin resistance. *J Clin Invest* **106**, 473-481. doi: 10.1172/JCI10842

Kang, L., Zhang, X., Ji, L., Kou, T., Smith, S.M., Zhao, B., Guo, X., Pineda-Torra, I., Wu, L., and Hu, X. 2020. The colonic macrophage transcription factor RBP-J orchestrates intestinal immunity against bacterial pathogens. *J Exp Med* **217**. doi: 10.1084/jem.20190762

Kang, S.G., Liu, W.-H., Lu, P., Jin, H.Y., Lim, H.W., Shepherd, J., Fremgen, D., Verdin, E., Oldstone, M.B.A., Qi, H., Teijaro, J.R., and Xiao, C. 2013. MicroRNAs of the miR-17~92 family are critical regulators of TFH differentiation. *Nat Immunol* **14**, 849-857. doi: 10.1038/ni.2648

Kozomara, A., and Griffiths-Jones, S. 2014. miRBase: annotating high confidence microRNAs using deep sequencing data. *Nucleic Acids Res* **42**, D68-D73. doi: 10.1093/nar/gkt1181

Krol, J., Loedige, I., and Filipowicz, W. 2010. The widespread regulation of microRNA biogenesis, function and decay. *Nat Rev Genet* **11**, 597-610. doi: 10.1038/nrg2843

Kuleshov, M.V., Jones, M.R., Rouillard, A.D., Fernandez, N.F., Duan, Q., Wang, Z., Koplev, S., Jenkins, S.L., Jagodnik, K.M., Lachmann, A., McDermott, M.G., Monteiro,

549 C.D., Gundersen, G.W., and Ma'ayan, A. 2016. Enrichr: a comprehensive gene set
 550 enrichment analysis web server 2016 update. *Nucleic Acids Res* **44**, W90-W97. doi:
 551 10.1093/nar/gkw377
 552 Lai, M., Gonzalez-Martin, A., Cooper, A.B., Oda, H., Jin, H.Y., Shepherd, J., He, L.,
 553 Zhu, J., Nemazee, D., and Xiao, C. 2016. Regulation of B-cell development and
 554 tolerance by different members of the miR-17 ~ 92 family microRNAs. *Nat Commun*
 555 **7**, 12207. doi: 10.1038/ncomms12207
 556 Lee, D.-F., Kuo, H.-P., Chen, C.-T., Hsu, J.-M., Chou, C.-K., Wei, Y., Sun, H.-L., Li,
 557 L.-Y., Ping, B., Huang, W.-C., He, X., Hung, J.-Y., Lai, C.-C., Ding, Q., Su, J.-L., Yang,
 558 J.-Y., Sahin, A.A., Hortobagyi, G.N., Tsai, F.-J., Tsai, C.-H., and Hung, M.-C. 2007.
 559 IKK β Suppression of TSC1 Links Inflammation and Tumor Angiogenesis via the
 560 mTOR Pathway. *Cell* **130**, 440-455. doi: <https://doi.org/10.1016/j.cell.2007.05.058>
 561 Luche, H., Weber, O., Nageswara Rao, T., Blum, C., and Fehling, H.J. 2007. Faithful
 562 activation of an extra-bright red fluorescent protein in “knock-in” Cre-reporter mice
 563 ideally suited for lineage tracing studies. *Eur J Immunol* **37**, 43-53. doi:
 564 10.1002/eji.200636745
 565 Martin, M., Rehani, K., Jope, R.S., and Michalek, S.M. 2005. Toll-like receptor-
 566 mediated cytokine production is differentially regulated by glycogen synthase kinase 3.
 567 *Nat Immunol* **6**, 777-784. doi: 10.1038/ni1221
 568 Mendell, J.T. 2008. miRiad roles for the miR-17-92 cluster in development and disease.
 569 *Cell* **133**, 217-222. doi: 10.1016/j.cell.2008.04.001
 570 Mogilyansky, E., and Rigoutsos, I. 2013. The miR-17/92 cluster: a comprehensive
 571 update on its genomics, genetics, functions and increasingly important and numerous
 572 roles in health and disease. *Cell Death Differ* **20**, 1603. doi: 10.1038/cdd.2013.125
 573 Moore, K.W., Malefyt, R.d.W., Coffman, R.L., and O'Garra, A. 2001. Interleukin-10
 574 and the Interleukin-10 Receptor. *Annu Rev Immunol* **19**, 683-765. doi:
 575 10.1146/annurev.immunol.19.1.683
 576 Mosser, D.M., and Edwards, J.P. 2008. Exploring the full spectrum of macrophage
 577 activation. *Nat Rev Immunol* **8**, 958. doi: 10.1038/nri2448
 578 O'Donnell, K.A., Wentzel, E.A., Zeller, K.I., Dang, C.V., and Mendell, J.T. 2005. c-

579 Myc-regulated microRNAs modulate E2F1 expression. *Nature* **435**, 839-843. doi:
580 10.1038/nature03677

581 Odegaard, J.I., and Chawla, A. 2011. Alternative macrophage activation and
582 metabolism. *Annu Rev Pathol* **6**, 275-297. doi: 10.1146/annurev-pathol-011110-130138

583 Olefsky, J.M., and Glass, C.K. 2010. Macrophages, Inflammation, and Insulin
584 Resistance. *Annu Rev Physiol* **72**, 219-246. doi: 10.1146/annurev-physiol-021909-
585 135846

586 Ouyang, W., and O'Garra, A. 2019. IL-10 Family Cytokines IL-10 and IL-22: from
587 Basic Science to Clinical Translation. *Immunity* **50**, 871-891. doi:
588 10.1016/j.immuni.2019.03.020

589 Ouyang, W., Rutz, S., Crellin, N.K., Valdez, P.A., and Hymowitz, S.G. 2011. Regulation
590 and Functions of the IL-10 Family of Cytokines in Inflammation and Disease. *Annu*
591 *Rev Immunol* **29**, 71-109. doi: 10.1146/annurev-immunol-031210-101312

592 Ozes, O.N., Akca, H., Mayo, L.D., Gustin, J.A., Maehama, T., Dixon, J.E., and Donner,
593 D.B. 2001. A phosphatidylinositol 3-kinase/Akt/mTOR pathway mediates and PTEN
594 antagonizes tumor necrosis factor inhibition of insulin signaling through insulin
595 receptor substrate-1. *Proc Natl Acad Sci U S A* **98**, 4640-4645. doi:
596 10.1073/pnas.051042298

597 Qatanani, M., and Lazar, M.A. 2007. Mechanisms of obesity-associated insulin
598 resistance: many choices on the menu. *Genes Dev* **21**, 1443-1455. doi:
599 10.1101/gad.1550907

600 Saraiva, M., and O'Garra, A. 2010. The regulation of IL-10 production by immune cells.
601 *Nat Rev Immunol* **10**, 170-181. doi: 10.1038/nri2711

602 Shi, Y., Lee, J.-S., and Galvin, K.M. 1997. Everything you have ever wanted to know
603 about Yin Yang 1. *Biochim Biophys Acta* **1332**, F49-F66. doi:
604 [https://doi.org/10.1016/S0304-419X\(96\)00044-3](https://doi.org/10.1016/S0304-419X(96)00044-3)

605 Sugimoto, M.A., Vago, J.P., Perretti, M., and Teixeira, M.M. 2019. Mediators of the
606 Resolution of the Inflammatory Response. *Trends Immunol* **40**, 212-227. doi:
607 10.1016/j.it.2019.01.007

608 Ventura, A., Young, A.G., Winslow, M.M., Lintault, L., Meissner, A., Erkland, S.J.,

Newman, J., Bronson, R.T., Crowley, D., Stone, J.R., Jaenisch, R., Sharp, P.A., and
 Jacks, T. 2008. Targeted deletion reveals essential and overlapping functions of the
 miR-17 ~ 92 family of miRNA clusters. *Cell* **132**, 875-886. doi:
 10.1016/j.cell.2008.02.019

Wang, Q., Li, Y.C., Wang, J., Kong, J., Qi, Y., Quigg, R.J., and Li, X. 2008. miR-17-92
 cluster accelerates adipocyte differentiation by negatively regulating tumor-suppressor
 Rb2/p130. *Proc Natl Acad Sci U S A* **105**, 2889-2894. doi: 10.1073/pnas.0800178105

Xiao, C., Srinivasan, L., Calado, D.P., Patterson, H.C., Zhang, B., Wang, J., Henderson,
 J.M., Kutok, J.L., and Rajewsky, K. 2008. Lymphoproliferative disease and
 autoimmunity in mice with increased miR-17-92 expression in lymphocytes. *Nat*
Immunol **9**, 405-414. doi: 10.1038/ni1575

Xu, H., Zhu, J., Smith, S., Foldi, J., Zhao, B., Chung, A.Y., Outtz, H., Kitajewski, J.,
 Shi, C., Weber, S., Saftig, P., Li, Y., Ozato, K., Blobel, C.P., Ivashkiv, L.B., and Hu, X.
 2012. Notch-RBP-J signaling regulates the transcription factor IRF8 to promote
 inflammatory macrophage polarization. *Nat Immunol* **13**, 642-650. doi:
 10.1038/ni.2304

Yin, M.-J., Yamamoto, Y., and Gaynor, R.B. 1998. The anti-inflammatory agents aspirin
 and salicylate inhibit the activity of I κ B kinase- β . *Nature* **396**, 77-80. doi:
 10.1038/23948

Zhang, X., Li, X., Ning, F., Shang, Y., and Hu, X. 2019. TLE4 acts as a corepressor of
 Hes1 to inhibit inflammatory responses in macrophages. *Protein & Cell* **10**, 300-305.
 doi: 10.1007/s13238-018-0554-3

Zhang, X., Smith, S.M., Wang, X., Zhao, B., Wu, L., and Hu, X. 2020. Three paralogous
 clusters of the miR-17~92 family of microRNAs restrain IL-12-mediated immune
 defense. *Cell Mol Immunol*. doi: 10.1038/s41423-020-0363-5

Figure Legends

Figure 1. miR-17~92 family miRNAs protect mice from obesity.

(A) A representative photograph (left panel) and body weight (right panel) of the *Lyz2-Cre* (WT) and *miR-106a~363^{-/-} miR-106b~25^{-/-} miR-17~92^{fllox/fllox} Lyz2-Cre* (TKO) mice at the age of 30 weeks, n=14-16 per group. (B and C) Visceral adipose tissue (VAT) weight (B) and VAT percentage of body weight (C) of WT and TKO mice at the age of 30 weeks. (D and E) Total adipose tissue weight (D) and its percentage of body weight (E) of WT and TKO mice at the age of 30 weeks. (F-J) WT and TKO mice were fed with a high-fat diet and were sacrificed on 13-20 weeks post high-fat diet. Body weight of each mouse was measured weekly, n=8 per group (F); VAT weight (G) and VAT percentage of body weight (H) were measured; total adipose tissue weight (I) and its percentage of body weight (J) were measured by scanning the whole mice with magnetic resonance imaging (MRI) machine. (K-O) C57BL/6J mice were irradiated and transferred with WT (WT → WT) or TKO (TKO → WT) bone marrows. Then these bone marrow (BM) chimeras were fed with a high-fat diet and were sacrificed on 16-28 weeks post high-fat diet. Body weight of each mouse was measured weekly, n=7-8 per group (K); VAT weight (L), VAT percentage of body weight (M), total adipose tissue weight (N) and its percentage of body weight (O) were measured. **P*<0.05, ***P*<0.01, ****P*<0.001, and *****P*<0.0001 (unpaired Student's *t*-test). Data are pooled from four (A-C), two (D,E,F,K,L and M), or five (G and H) independent experiments (mean ± s.e.m.), or are representative of one independent experiment (I,J,N and O).

Figure 1-figure supplement 1. Schematic representation of the miR-17~92 family miRNAs.

(A and B) Schematic representation of three miRNA clusters of miR-17~92 family miRNAs (A) and their target sequences (B). The mature miRNAs in different families are shown in different colors. Yellow: members of the miR-17 family; Red: members of the miR-18 family; Blue: members of the miR-19 family; Green: members of the miR-25 family. The 'seed region' of each mature miRNA is shown in bold format.

Figure 1-figure supplement 2. The miR-17~92 family miRNAs are efficiently deleted in TKO BMDMs. (A-C) qPCR analysis of various mature miRNAs (horizontal axes) in the miR-17~92 cluster (A), miR-106a~363 cluster (B), and miR-106b~25 cluster (C) in *Lyz2*-Cre (WT) and miR-106a~363^{-/-} miR-106b~25^{-/-} miR-17~92^{flx/flx} *Lyz2*-Cre (TKO) BMDMs; results are presented as relative expression normalized to the control small RNA U6. Data are representative of two independent experiments (mean + s.d.).

Figure 1-figure supplement 3. miR-17~92 family miRNAs protect mice from obesity. (A-B) Body weights of the *Lyz2*-Cre (WT) and TKO male (A) or female (B) mice at the age of 30 weeks (n=7-9 per group). (C) Body weights of WT and TKO mice fed with regular chow diet, n=4 per group. (D) Brown adipose tissue (BAT) weights of WT and TKO mice at the age of 30 weeks. (E) CD45.1 mice were irradiated and transferred with 10⁶ donor bone marrow (BM) cells from WT (WT → WT) or TKO (TKO → WT) mice. 6 weeks post BM transfer, CD45.1 and CD45.2 expression on adipose tissue macrophages (ATMs) was analyzed by flow cytometry. One representative experiment was shown in the left panel and cumulative data were shown in the right panel (n=4 per group). (F) Body weights of chimeric mice transferred with WT (WT → WT) or TKO (TKO → WT) bone marrows fed with regular chow diet (n=8 per group). Each symbol represents an individual mouse. **P*<0.05, ***P*<0.01 and *****P*<0.0001 (unpaired Student's *t*-test). Data are representative or are pooled from two (A,B,D and E) or one (C and F) independent experiments (mean ± s.e.m).

Figure 2. miR-17~92 family miRNAs maintain adipose tissue macrophage homeostasis.

(A) Glucose tolerance test in WT and TKO mice (left panel); area under curve (AUC) of left panel (right panel), n=6 per group. (B) qPCR analysis of *Tnf* and *Il10* mRNA in visceral adipose tissue of WT and TKO mice (C and D) Flow cytometry of adipose tissue macrophage (ATM) population in WT and TKO mice. (C) A representative figure showing the ATM population of CD45⁺ cells; (D) cumulative quantification of ATM as

in (C). (E and F) ATMs were sorted from WT and TKO mice fed with regular chow diet, RNA samples of ATMs were extracted and pooled from two mice, and genome wide RNA profiling analyses were performed. (E) Gene Ontology analysis of WT and TKO ATM RNA-seq datasets showing the enriched gene ontology terms in TKO ATMs; (F) RNA-seq analysis showing RNA expression in TKO ATMs versus those in WT cells. RNAs up-regulated in TKO ATMs were colored red, whereas RNAs down-regulated were colored blue, gene *Tnf* was pointed out and colored orange and gene *Il10* was pointed out and colored green. Top 10 up-regulated genes (*Ighg2b*, *Gm11843*, *Dcdc2a*, *Mmp7*, *Slc38a5*, *Tenm2*, *Cdh16*, *Ptn*, *Ighv1-42*, *Nanp*) were colored yellow and top 10 down-regulated genes (*Csf2ra*, *Zfp125*, *Cxcl5*, *Ighv14-3*, *Igkv4-59*, *Igkv6-20*, *Igkv16-104*, *Fth-ps2*, *Igkv4-91*, *B230303A05Rik*) were colored bright blue. (G and H) qPCR analysis of *Tnf* (G) and *Il10* (H) mRNA in ATMs of WT and TKO mice. Results were shown as relative expression normalized to those expressions in one WT mice of each experiment. NS, not significant ($P>0.05$); $*P<0.05$, $***P<0.001$, and $****P<0.0001$ (unpaired Student's *t*-test). Data are representative of three independent experiments (C) or are pooled from two (A), three (B,D) or five (G,H) independent experiments (mean \pm s.e.m).

Figure 2-figure supplement 1. miR-17~92 family miRNAs inhibit TNF and promote IL-10 expression in adipose tissue. (A and B) Protein levels of TNF (A) and IL-10 (B) in serum of WT and TKO mice measured by ELISA. (C and D) qPCR analysis of *Tnf* (C) and *Il10* (D) mRNA with additional primer pairs in WT and TKO adipose tissues. $*P<0.05$, $**P<0.01$ (unpaired Student's *t*-test). Data are pooled from three (A-D) independent experiments (mean \pm s.e.m.).

Figure 2-figure supplement 2. The miR-17~92 family miRNAs are efficiently deleted in TKO ATMs. (A and B) Flow cytometry analysis of RFP expression in adipose tissue macrophages (A) and peritoneal macrophages (B, positive control) from *Lyz2*-Cre and *Lyz2*-RFP mice. (C-E) qPCR analysis of various mature miRNAs (horizontal axes) in the miR-17~92 cluster (C), miR-106a~363 cluster (D), and miR-

106b~25 cluster (E) in *Ly2z*-Cre (WT) and *miR-106a~363^{-/-} miR-106b~25^{-/-} miR-17~92^{flx/flx}* *Ly2z*-Cre (TKO) ATMs; results are presented as relative expression normalized to the control small RNA U6. Data are representative of two independent experiments (mean + s.d.).

Figure 2-figure supplement 3. The ATM populations are not changed in TKO mice.

(A-E) Flow cytometry analysis of CD11c (A), CD64 (B), CX₃CR1 (C), MerTK (D) and Ly6C (E) expression in adipose tissue macrophages from *Ly2z*-Cre (WT) and *miR-106a~363^{-/-} miR-106b~25^{-/-} miR-17~92^{flx/flx}* *Ly2z*-Cre (TKO) mice. Data are representative of two independent experiments.

Figure 2-figure supplement 4. Adipose tissue macrophages in TKO mice are more inflammatory.

(A and B) WT and TKO mice were fed with regular chow diet or high fat diet (HFD) for 8 weeks, ATMs were sorted for a genome wide RNA profiling analysis. (A) Gene Ontology analysis of RNA-seq datasets of ATMs from WT mice fed with chow diet or HFD. (B) Inflammatory score of WT and TKO mice fed with chow diet or HFD. Inflammatory score = sum of log (FPKM+1) of representative pro-inflammatory genes (*Tnf*, *Il6*, *Cxcl1*, *Ccl2* and *Ccl8*) - sum of log (FPKM+1) of representative anti-inflammatory genes (*Il10*, *Il4*, *Il5* and *Il13*). (C and D) qPCR analysis of *Tnf* (C) and *Il10* (D) mRNA with an additional set of primers in WT and TKO ATMs. **P*<0.05 (unpaired Student's *t*-test). Data are representative of one (A and B) or are pooled from two (C,D) independent experiments (mean ± s.e.m.).

Figure 3. miR-17~92 family miRNAs balance the production of TNF and IL-10 in macrophages.

(A and B) qPCR analysis of *Tnf* (A) and *Il10* (B) mRNA in WT and TKO BMDMs without stimulation. (C and D) qPCR analysis of *Tnf* (C) and *Il10* (D) mRNA in WT and TKO BMDMs stimulated for the indicated periods with LPS. (E and F) ELISA of TNF (E) and IL-10 (F) in supernatants from WT and TKO BMDMs stimulated for the indicated periods with LPS. (G) ELISA of TNF in supernatants from WT and TKO

BMDMs pre-treated 1 h with indicated dose of IL-10 and then stimulated with LPS for 6 h. **(H)** WT and TKO mice were injected with PBS or anti-TNF (10 mg/kg) weekly and were fed with a high-fat diet. Body weight of each mice was measured weekly. NS, not significant ($P>0.05$); $*P<0.05$, $**P<0.01$ and $***P<0.001$ (paired Student's *t*-test and two-way ANOVA). Data are representative of or are pooled from five (**A-D**), four (**E,F**), three (**G**) or one (**H**) independent experiments (mean + s.d. in **A-G** and mean \pm s.e.m in **H**).

Figure 3-figure supplement 1. miR-17~92 family miRNAs balance the production of TNF and IL-10 in macrophages.

(A and B) qPCR analysis of *Tnf* (A) and *Il10* (B) mRNA with an additional set of primers in WT and TKO BMDMs without stimulation. (C and D) qPCR analysis of *Tnf* (C) and *Il10* (D) mRNA with an additional set of primers in WT and TKO BMDMs stimulated for the indicated periods with LPS. (E and F) qPCR analysis of *Tnf* (E) and *Il10* (F) mRNA in WT and TKO BMDMs stimulated for the indicated periods with Pam3CSK4. (G) ELISA of TNF in supernatants from WT and TKO BMDMs pre-treated 0.5 h with anti-IL-10R or anti-IgG (2 μ g/ml) and then stimulated with LPS for 6 h. NS, not significant ($P>0.05$); $*P<0.05$ (paired Student's *t*-test). Data are representative of five (A-D) or two (E and F) (mean + s.d.) or are pooled from four (G) independent experiments (mean + s.e.m.).

Figure 4. Three clusters of miR-17~92 family miRNAs regulate the expression of TNF and IL-10 collectively in macrophages.

(**A-D**) qPCR analysis of *Tnf* mRNA in WT and miR-17~92^{flox/flox} *Ly2z2-Cre* (17/92 KO) (**A**), miR-106a~363^{-/-} (106a KO) (**B**), miR-106b~25^{-/-} (106b KO) (**C**), or miR-106a~363^{-/-} miR-106b~25^{-/-} (106a 106b DKO) (**D**) BMDMs stimulated for the indicated periods with LPS. (**E-H**) qPCR analysis of *Il10* mRNA in WT and 17/92 KO (**E**), 106a KO (**F**), 106b KO (**G**), or 106a 106b DKO (**H**) BMDMs stimulated for the indicated periods with LPS. (**I and J**) qPCR analysis of *Tnf* (**I**) and *Il10* (**J**) mRNA in WT and various knockout (horizontal axes) BMDMs stimulated for 1 h with LPS;

results are presented relative to those of LPS-stimulated WT BMDMs. $**P<0.01$ (paired Student's *t*-test). Data are representative of two (A-C, E-G) or three (D and H) independent experiments or are pooled from two to three (I and J) independent experiments (mean + s.d.).

Figure 5. miR-17~92 family miRNAs promote the expression of Fos in macrophages.

(A) RNA-seq analysis showing RNA expression in TKO BMDMs versus those in WT cells. RNAs up-regulated in TKO BMDMs were colored red, whereas RNAs down-regulated were colored blue, gene *Fos* was pointed out and colored bright blue, gene *Phlpp2*, *E2f1*, *Pten* and *Bim* were pointed out and colored green. Top 10 up-regulated genes (*Atp6v0c-ps2*, *Hmgal-rs1*, *H2-Q6*, *H2-Ea-ps*, *Gm8580*, *Gm8909*, *Sap25*, *LOC547349*, *H2-L*, *H2-Q10*) were colored yellow and top 10 down-regulated genes (*Mir8114*, *0610010B08Rik*, *Gm14430*, *Gm8615*, *Asb4*, *Gm14305*, *6230416C02Rik*, *Gm38431*, *Pira7*, *Cpt1b*) were colored purple. (B and C) qPCR analysis of *Fos* mRNA in WT and TKO BMDMs stimulated for the indicated periods with LPS. (D) Immunoblotting analysis of c-Fos and p38 (loading control) in whole-cell lysates of WT and TKO BMDMs treated for the indicated periods with LPS. (E) Quantifications of c-Fos protein abundance in unstimulated condition in (D) by densitometry from four independent experiments. (F) qPCR analysis of *Il10* mRNA in WT and TKO BMDMs transfected with control or Fos overexpression vector and stimulated for the indicated periods with LPS. (G) Cumulative results from three independent experiments of *Il10* levels in LPS-stimulated 6 h results as in (F), normalized to mRNA expression in control vector transfected WT cells. (H) ELISA of IL-10 in supernatants from WT and TKO BMDMs transfected with control or Fos overexpression vector and stimulated with LPS for 12 h. $*P<0.05$ and $**P<0.01$ (paired Student's *t*-test). Data are representative of six (B), four (D) or three (F) independent experiments or are pooled from six (C), four (E) or three (G and H) independent experiments (mean + s.d.).

Figure 5-figure supplement 1. The regulation of TNF and IL-10 by miR-17~92

family miRNAs is independent of PTEN.

(A and B) qPCR analysis of *Tnf* (A) and *Il10* (B) mRNA in WT and TKO BMDMs stimulated with or without LPS for 3 h in the presence or absence of a PTEN inhibitor SF1670 (2 μ M). Data are representative of three independent experiments (mean + s.d.)

Figure 5-figure supplement 2. miR-17~92 family miRNAs sustain Fos expression in TKO BMDMs.

(A and B) The whole immunoblots of c-Fos (A) and p38 (B) in whole-cell lysates of WT and TKO BMDMs treated for the indicated periods with LPS.

Figure 5-figure supplement 3. The expression of Jun is comparable between WT and TKO BMDMs.

(A) qPCR analysis of *Jun* mRNA in WT and TKO BMDMs stimulated for the indicated periods with LPS. (B) Immunoblotting analysis of c-Jun and p38 (loading control) in whole-cell lysates of WT and TKO BMDMs treated for the indicated periods with LPS. Data are representative of two independent experiments (mean + s.d.).

Figure 5-figure supplement 4. Overexpression of Fos reduces the expression of TNF in TKO BMDMs.

(A and B) qPCR analysis of *Fos* (A) and *Tnf* (B) mRNA in WT and TKO BMDMs transfected with control or Fos overexpression vector and stimulated with or without LPS for 6h. Data are representative of three independent experiments (mean + s.d.).

Figure 6. miR-17~92 family miRNAs target YY1 to promote Fos expression in macrophages.

(A) qPCR analysis of *Yy1* mRNA in WT and TKO BMDMs stimulated for the indicated periods with LPS. (B) Immunoblotting analysis of YY1 and p38 (loading control) in whole-cell lysates of WT and TKO BMDMs treated for the indicated periods with LPS. (C) Quantifications of YY1 protein abundance in unstimulated condition in (B) by densitometry from three independent experiments. (D) Schematic illustration of predicted binding sites of miR-17 family miRNAs (red) in wild-type (YY1-WT) or

mutated (YY1-Mut) *Yy1* 3' untranslated region (UTR). (E) Luciferase reporter assays of *Rluc* gene expression containing the wild-type or mutated binding sites (as in D) in *Yy1* 3'UTR in 293T cells co-transfected with the luciferase reporter vector and negative control (Control), miR-17~92 cluster (17/92), miR-106a~363 cluster (106a), or miR-106b~25 cluster (106b) miRNAs overexpression vector. Results are presented as *Rluc*/Luc activity ratio and are normalized to values in the control vector group. (F) qPCR analysis of *Fos* mRNA in TKO BMDMs transfected with control or YY1 short interfering RNAs (siRNAs), normalized to mRNA expression in control siRNA transfected cells. (G) Immunoblotting analysis of c-Fos and p38 (loading control) in whole-cell lysates of TKO BMDMs transfected with control or YY1 siRNAs. (H) Quantifications of c-Fos protein abundance in (G) by densitometry from four independent experiments. (I and J) qPCR analysis of *Tnf* (I) and *Il10* (J) mRNA in TKO BMDMs transfected with control or YY1 siRNAs. (K and L) ELISA of TNF (K) and IL-10 (L) in supernatants from TKO BMDMs transfected with control or YY1 siRNAs. * $P < 0.05$ and ** $P < 0.01$ (paired Student's *t*-test). Data are representative of three (A, B, I and J) or four (G) independent experiments or are pooled from three (C, K and L), six (E) or four (F and H) independent experiments (mean + s.e.m.).

Figure 6-figure supplement 1. YY1 expression is efficiently knocked down by RNA interference.

(A) qPCR analysis of *Yy1* in WT BMDMs transfected with control or YY1 siRNAs, normalized to mRNA expression in control siRNA transfected cells. (B and C) qPCR analysis of *Yy1* (B) and immunoblotting analysis of YY1 and p38 (loading control, C) in TKO BMDMs transfected with control or YY1 siRNAs, qPCR results were normalized to mRNA expression in control siRNA transfected cells. ** $P < 0.01$ (paired Student's *t*-test). Data are pooled from (A) or are representative of (B) four independent experiments (mean + s.d.).

Figure 6-figure supplement 2. Fos is up-regulated after knocking down YY1 in WT BMDMs.

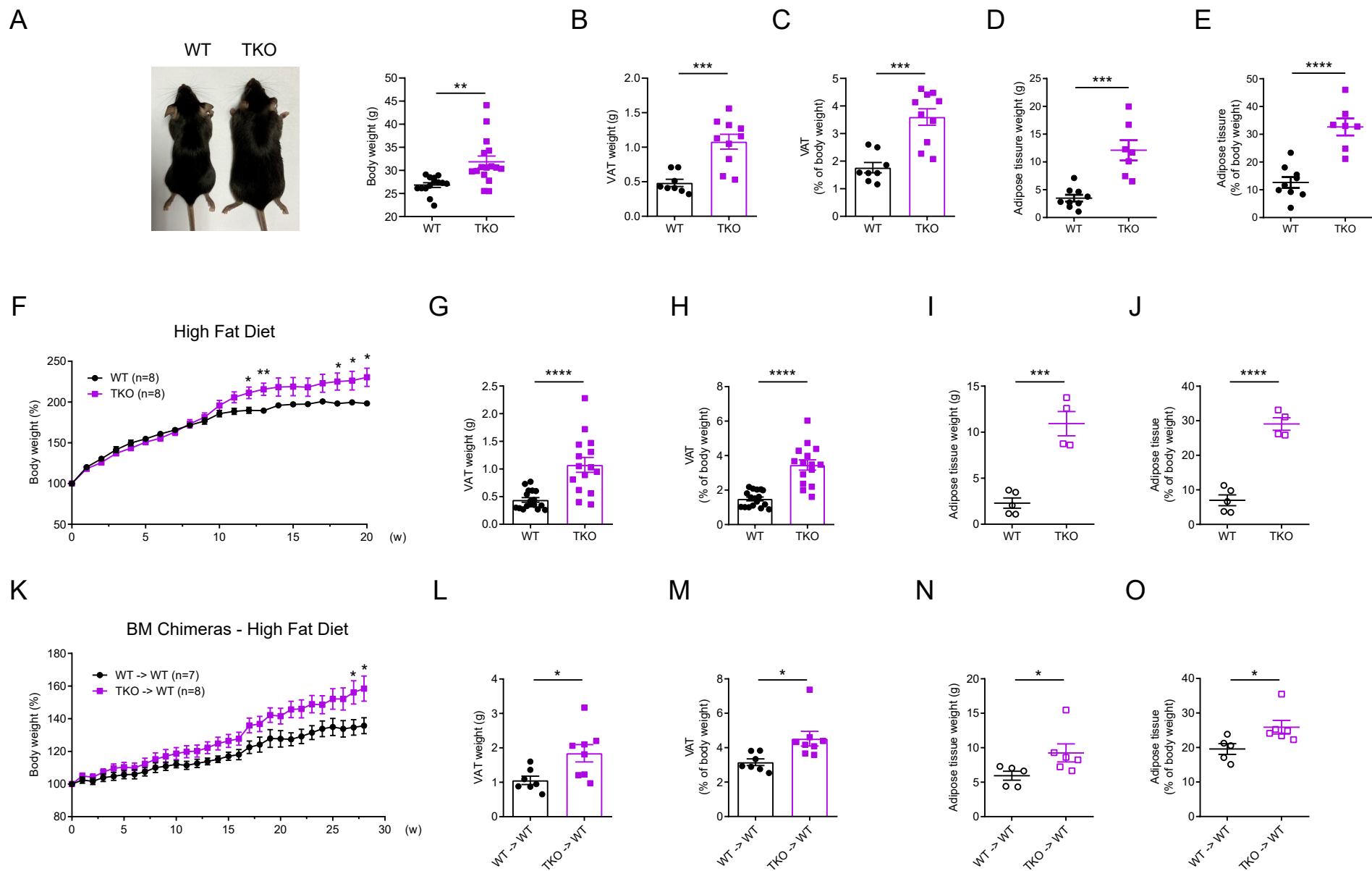
(A and B) qPCR analysis of *Fos* (A) and immunoblotting analysis of c-Fos and p38 (loading control, B) in WT BMDMs transfected with control or YY1 siRNAs. Data are representative of two independent experiments (mean + s.d.).

Figure 6-figure supplement 3. A model depicting functions and mechanisms of action of miR-17~92 family miRNAs in adipose tissue macrophages.

MicroRNAs of miR-17~92 family target YY1 to release its repression on Fos, allowing optimal production of IL-10 and subsequently repress production of TNF, thus inhibiting chronic inflammation such as obesity. Overall, miR-17~92 family miRNAs act as crucial regulators of the balance between pro- and anti-inflammatory cytokines in macrophages to maintain adipose tissue homeostasis.

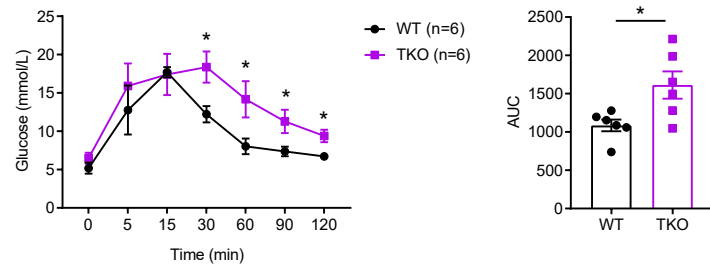
Supplementary file 1. Primers used in this study

Supplementary file 2. *Yy1* 3'UTR cloned fragments with miR-17 family miRNAs binding sites for luciferase reporter assays.

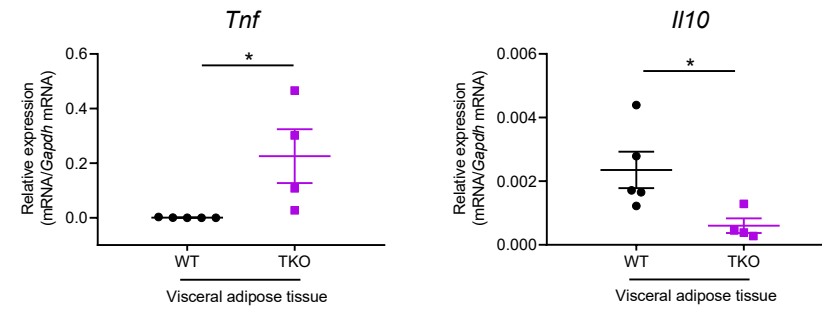


Zhang *et al.* Figure 1

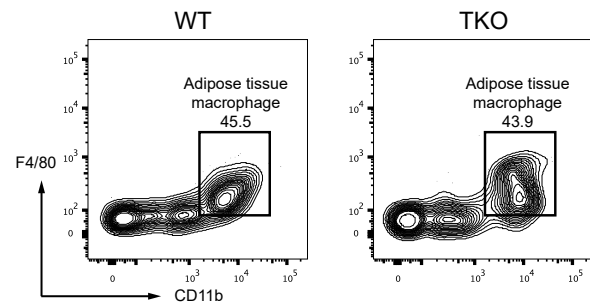
A



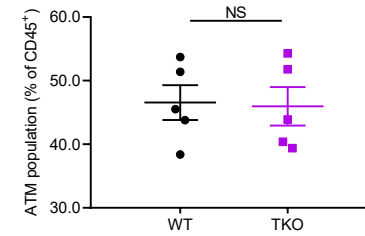
B



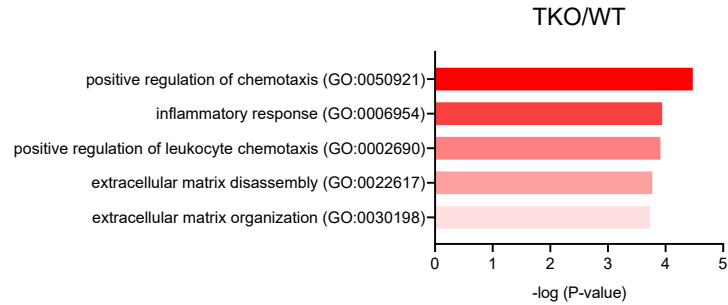
C



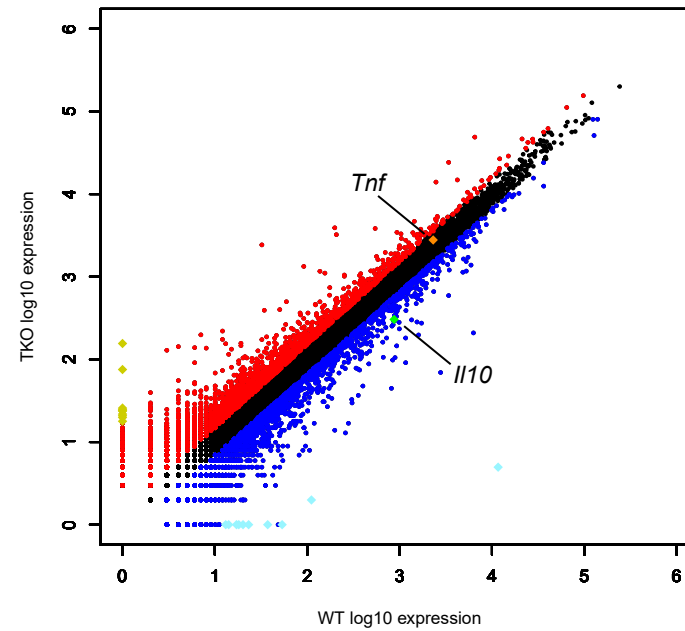
D



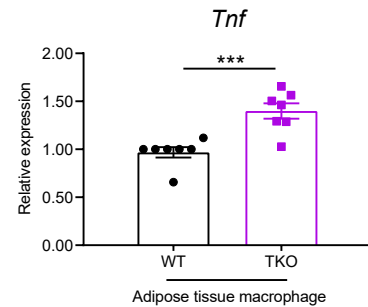
E



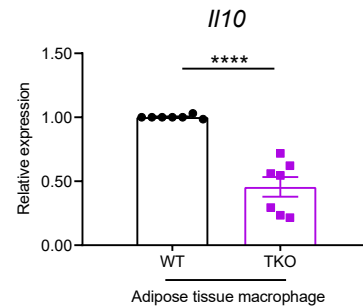
F

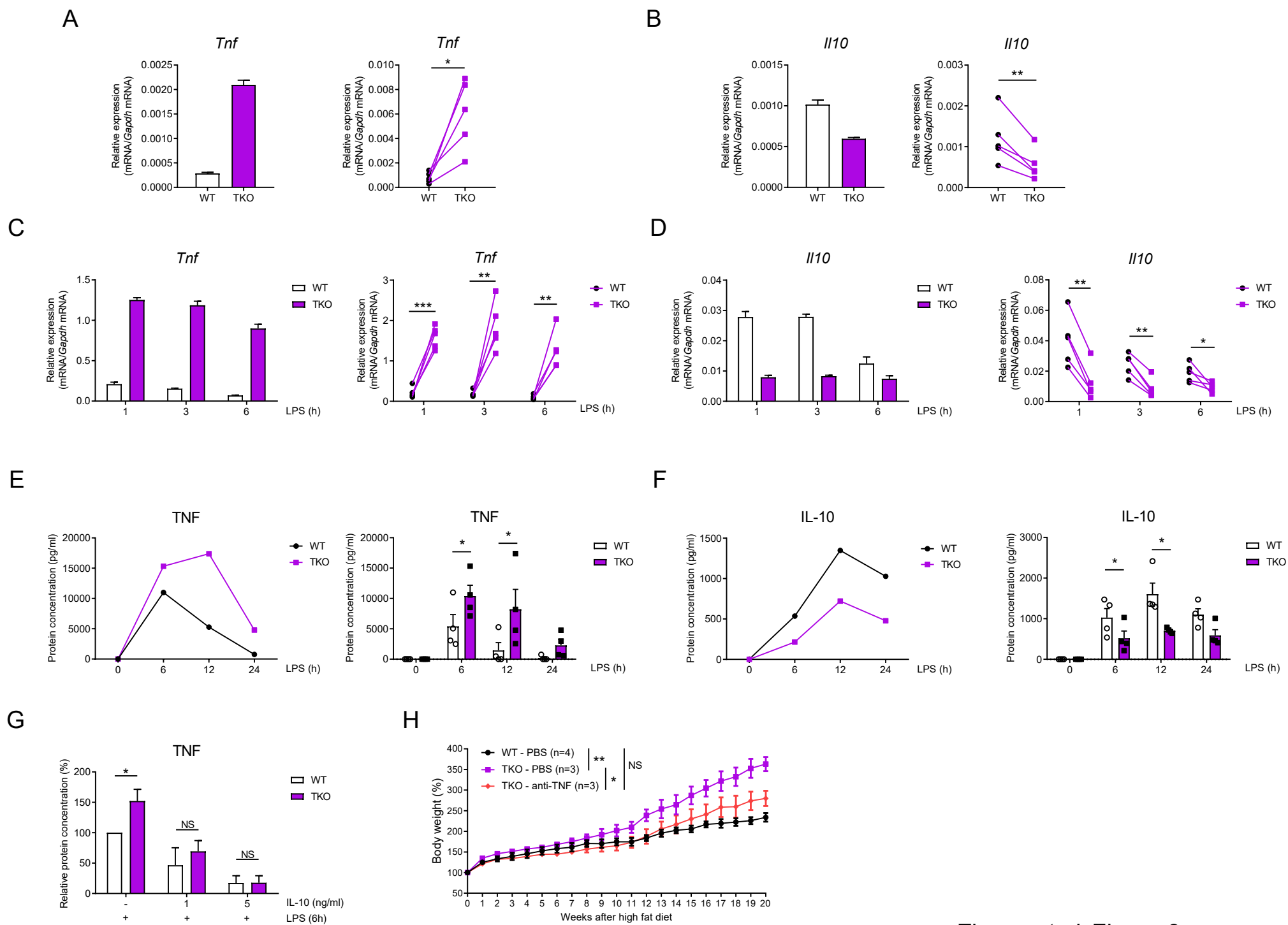


G



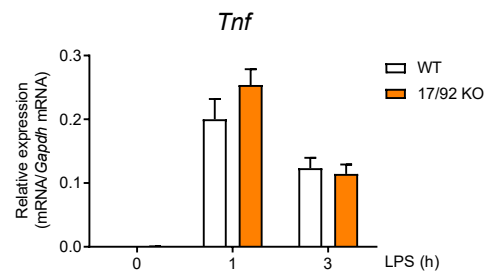
H



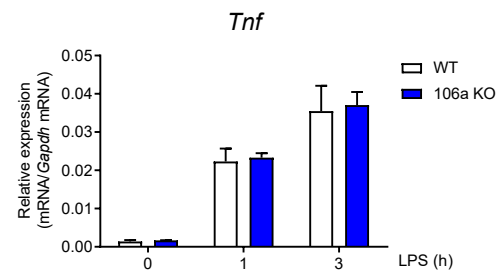


Zhang *et al.* Figure 3

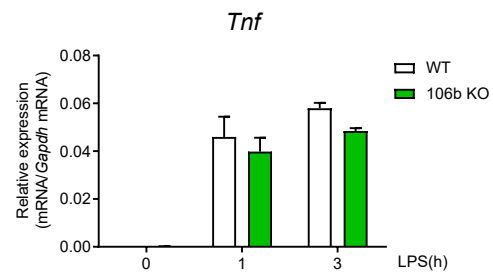
A



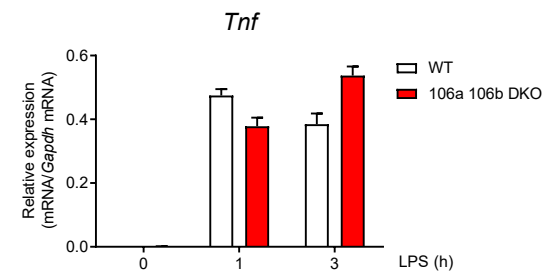
B



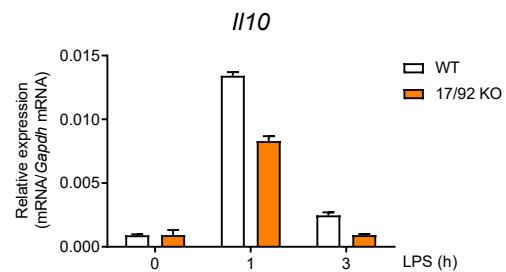
C



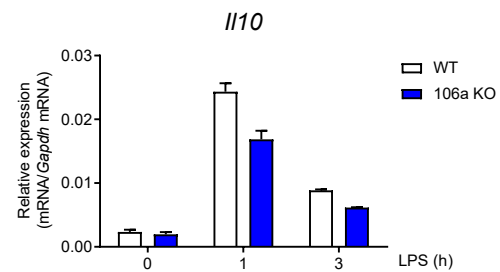
D



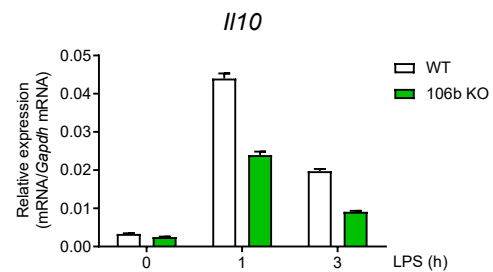
E



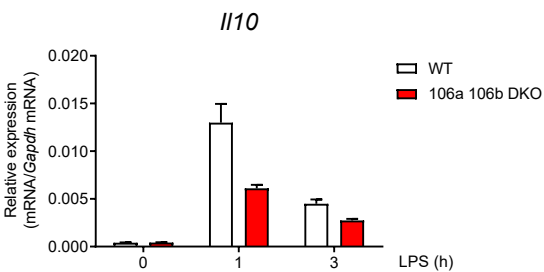
F



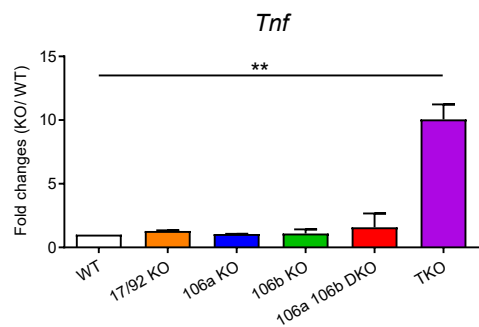
G



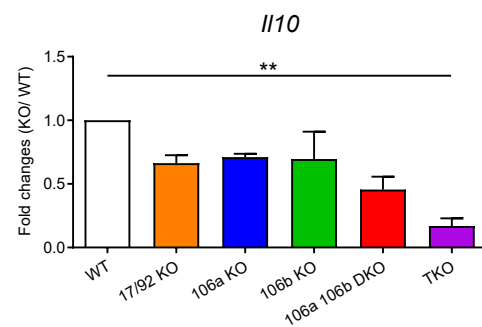
H

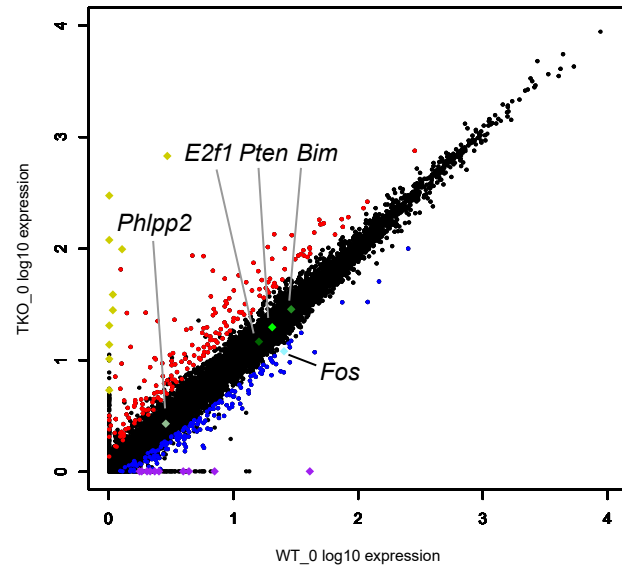
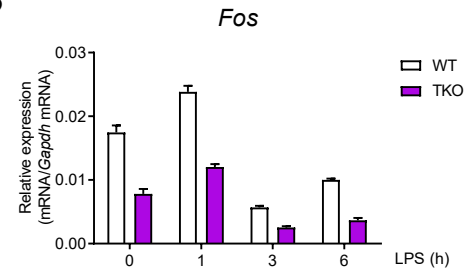
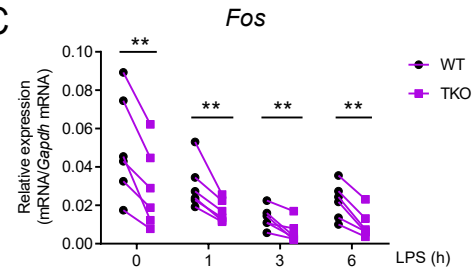
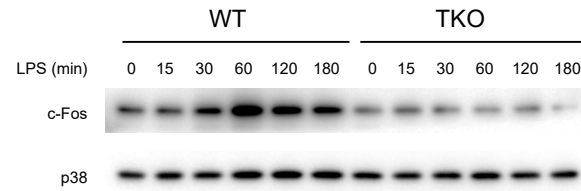
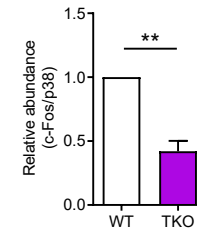
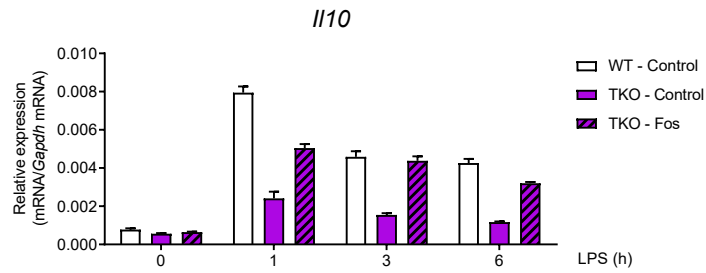
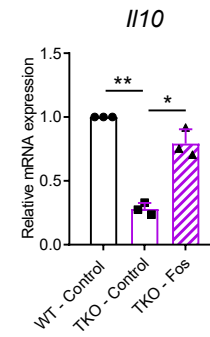
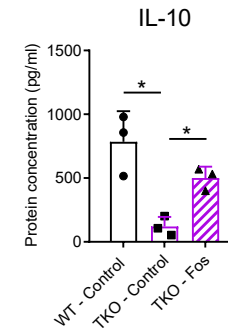


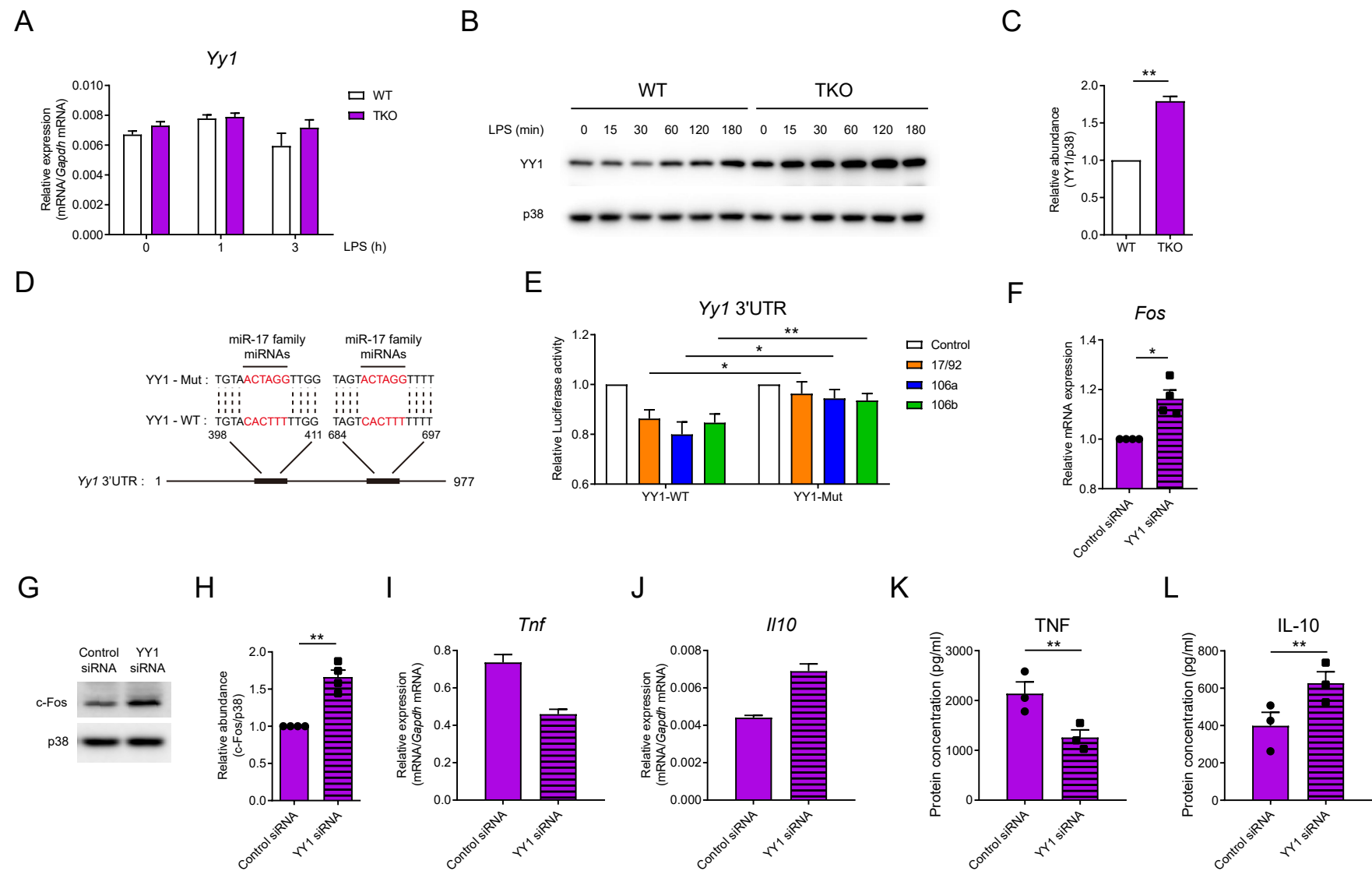
I



J

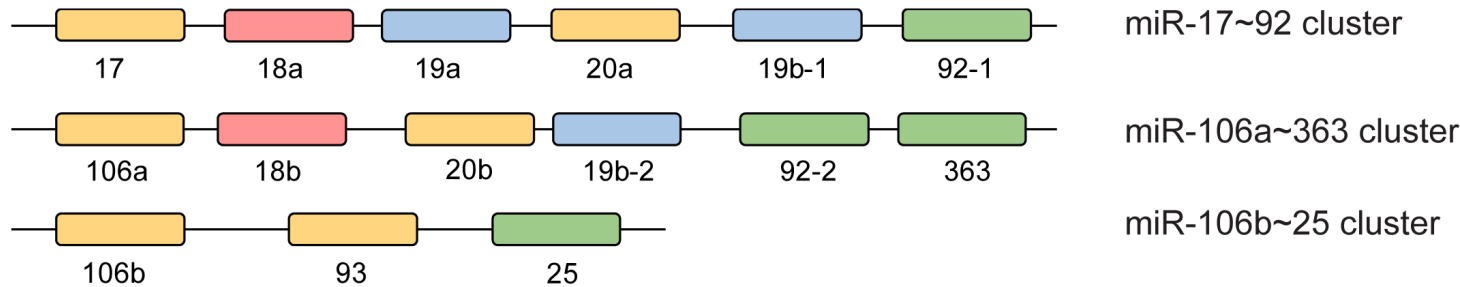


A**B****C****D****E****F****G****H**Zhang *et al.* Figure 5



Zhang *et al.* Figure 6

A

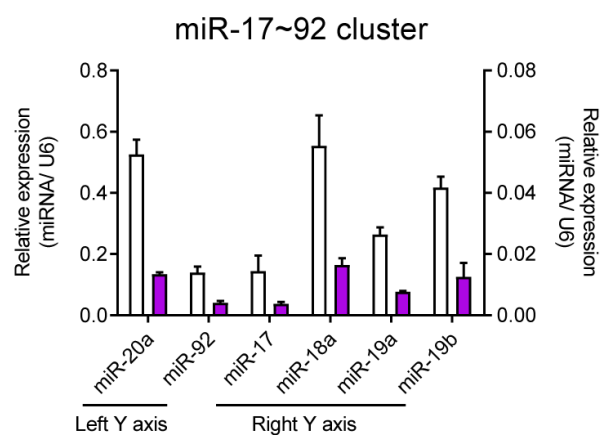


B

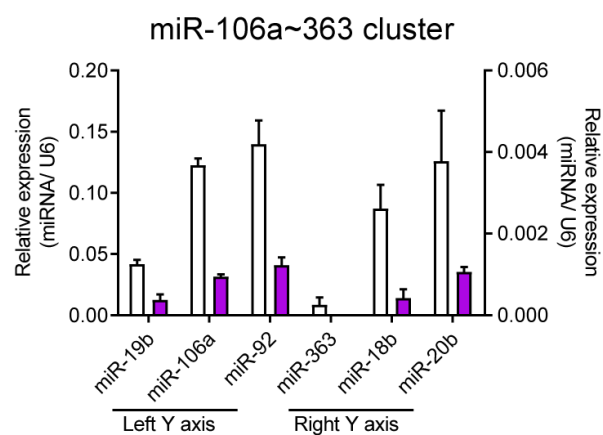
miR-17 family	17	CAAAGUG CUUACAGUGCAGGUAGU
	20a	UAAAGUG CUUAUAGUGCAGGUAG
	20b	CAAAGUG CUCAUAGUGCAGGUA
	106a	CAAAGUG CUAACAGUGCAGGUA
	106b	UAAAGUG CUGACAGUGCAGAU
	93	CAAAGUG CUGUUCGUGCAGGUAG
miR-18 family	18a	UAAGGUG CAUCUAGUGCAGAU
	18b	UAAGGUG CAUCUAGUGCAGUUA
miR-19 family	19a	UGUGCAA AUCUAUGCAAACUGA
	19b-1	UGUGCAA AUCCAUGCAAACUGA
	19b-2	UGUGCAA AUCCAUGCAAACUGA
miR-25 family	92-1	UAUUGCAC UUGUCCCGGCCUG
	92-2	UAUUGCAC UUGUCCCGGCCUG
	25	CAUUGCAC UUGUCUCGGUCUGA
	363	AAUUGCAC GGUAUCCAUCUGUAA

Zhang *et al.* Figure 1-figure supplement 2

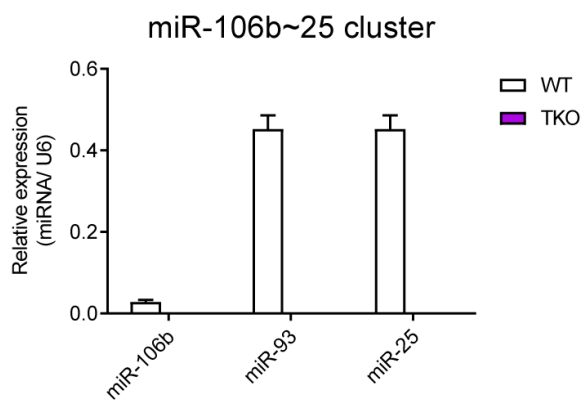
A



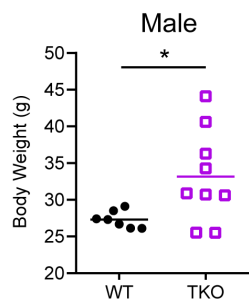
B



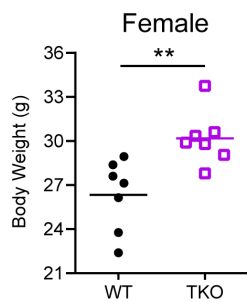
C



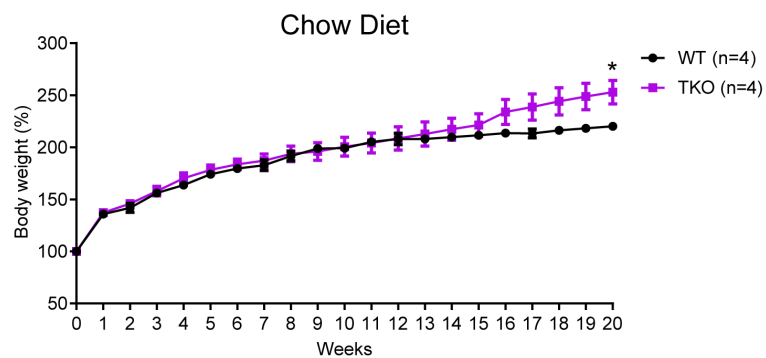
A



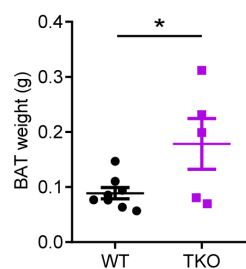
B



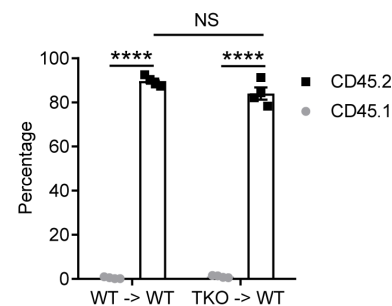
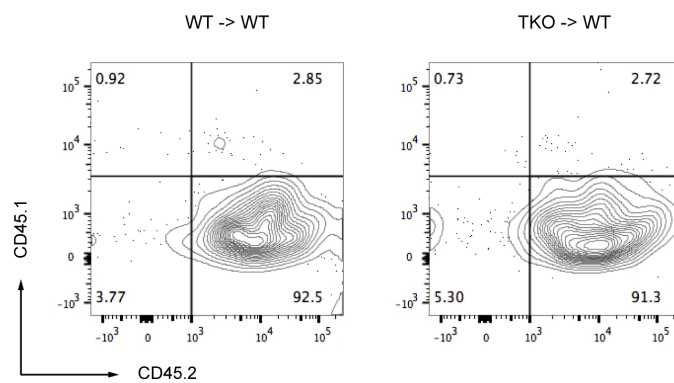
C



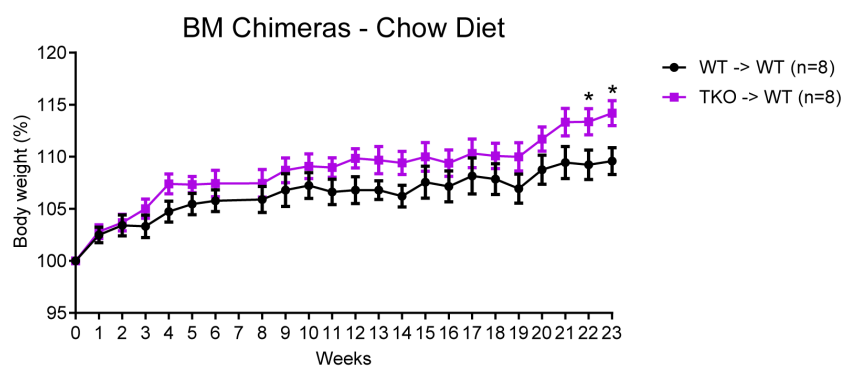
D

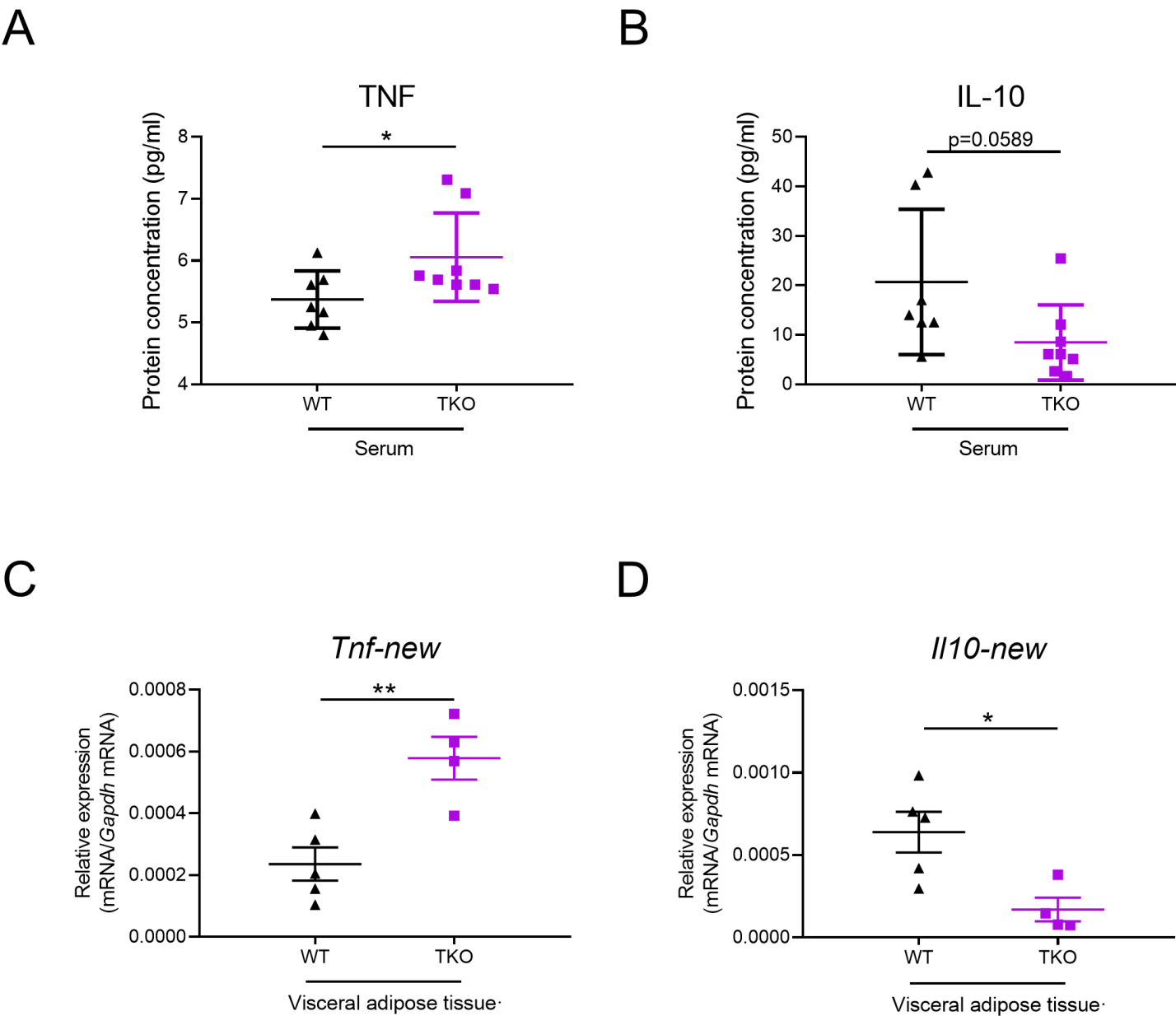


E



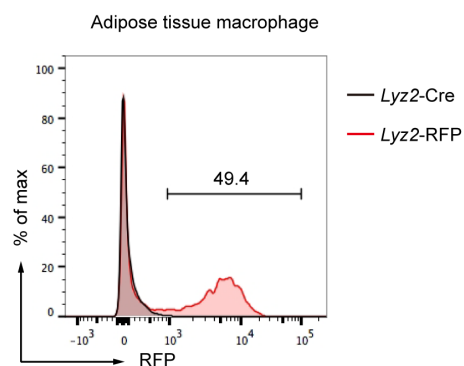
F



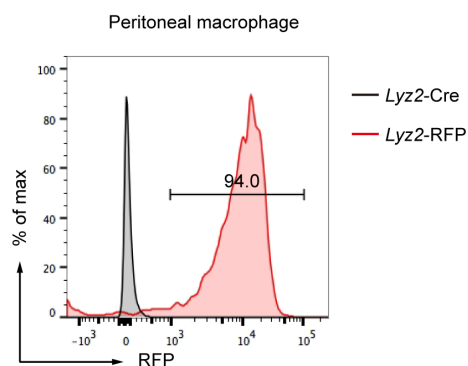


Zhang *et al.* Figure 2-figure supplement 2

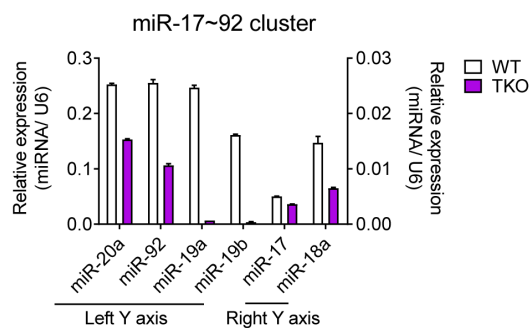
A



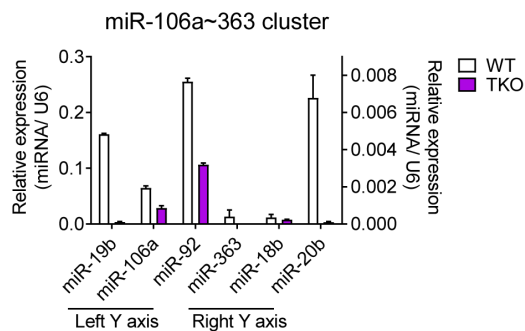
B



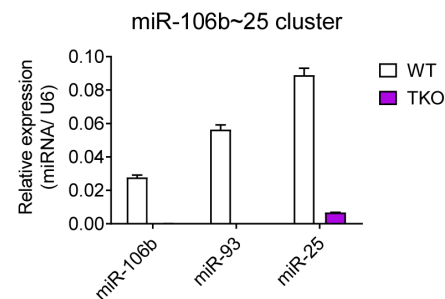
C



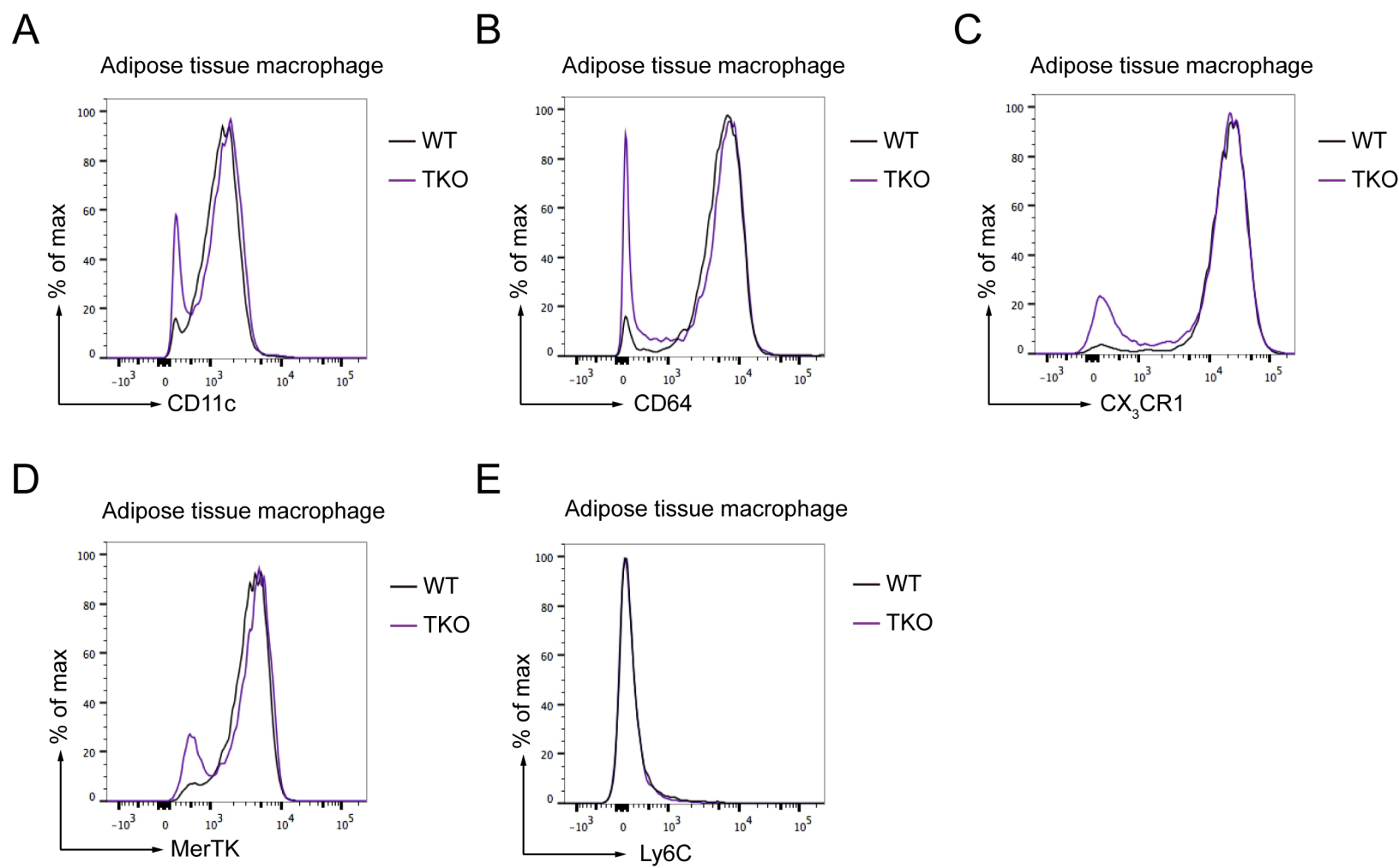
D



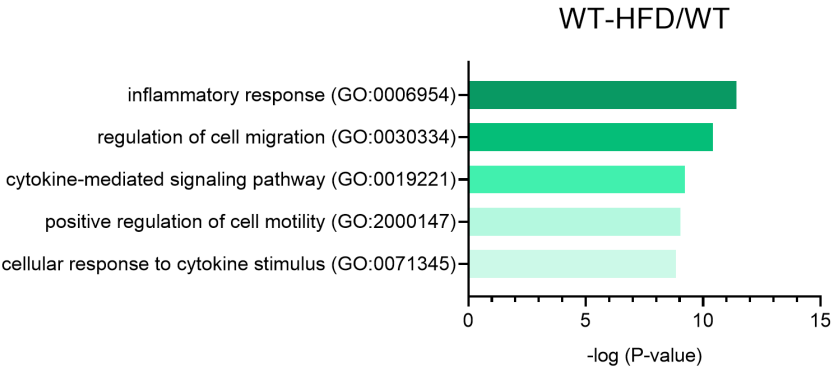
E



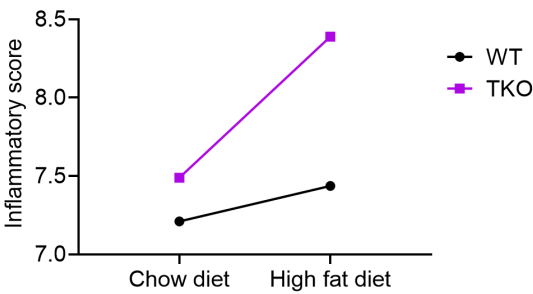
Zhang *et al.* Figure 2-figure supplement 3



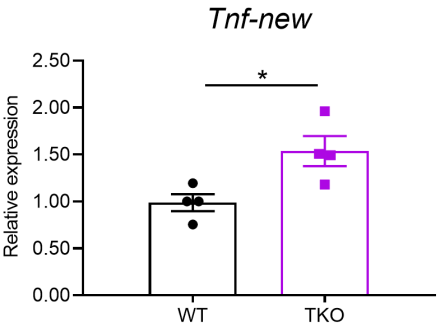
A



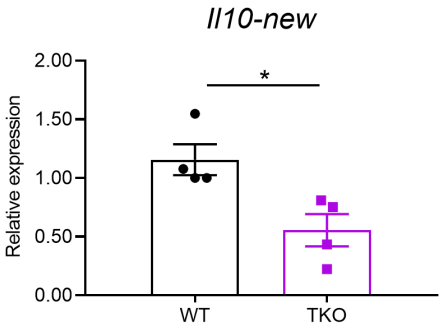
B



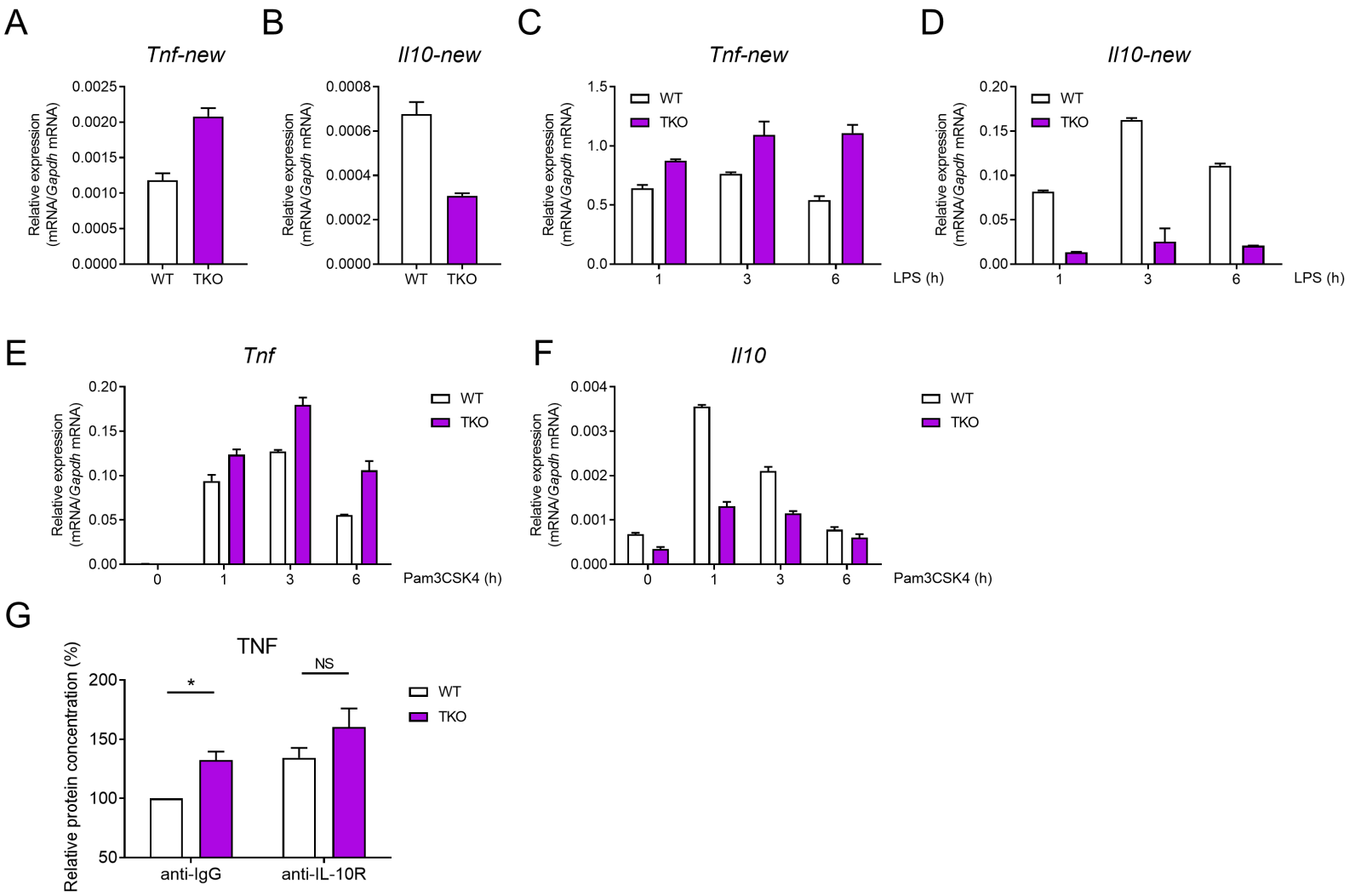
C



D

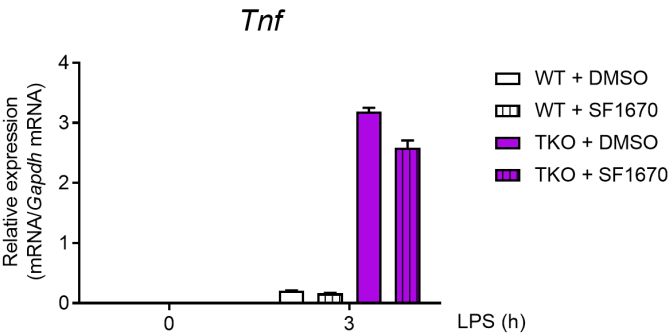


Zhang *et al.* Figure 3-figure supplement 1

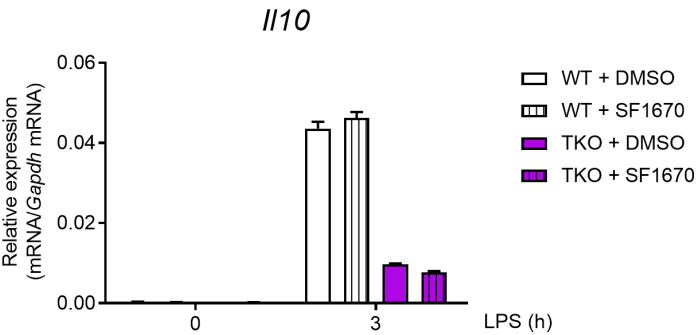


Zhang *et al.* Figure 5-figure supplement 1

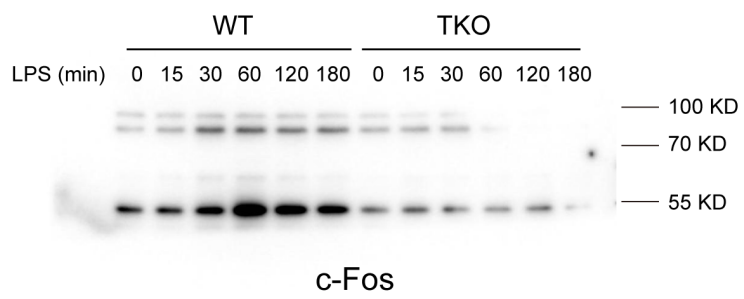
A



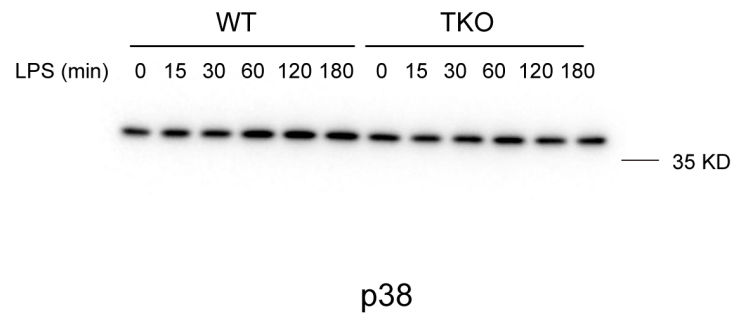
B



A

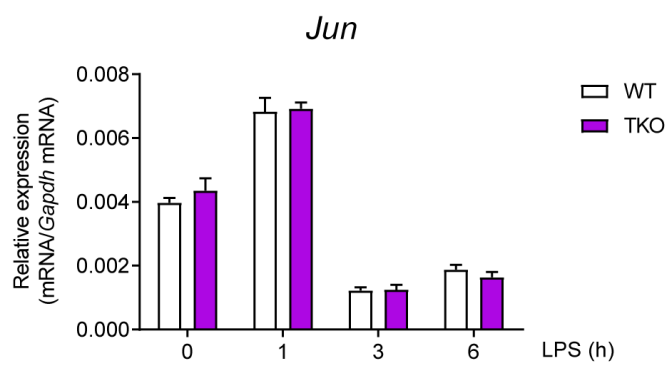


B

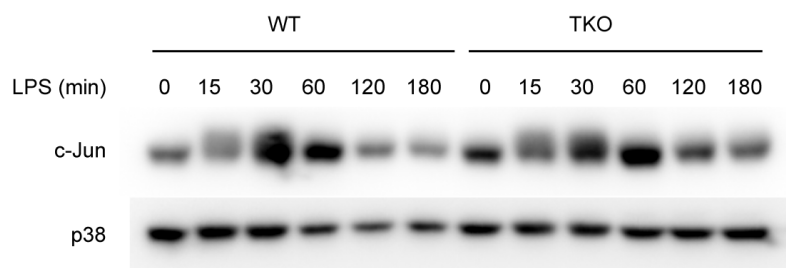


Zhang *et al.* Figure 5-figure supplement 3

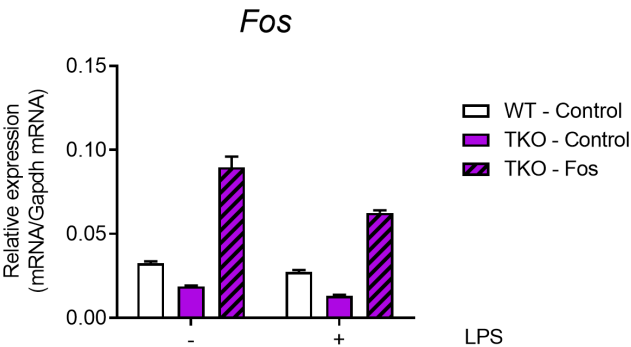
A



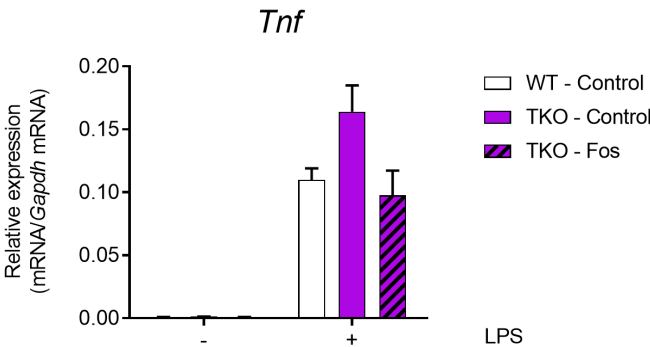
B



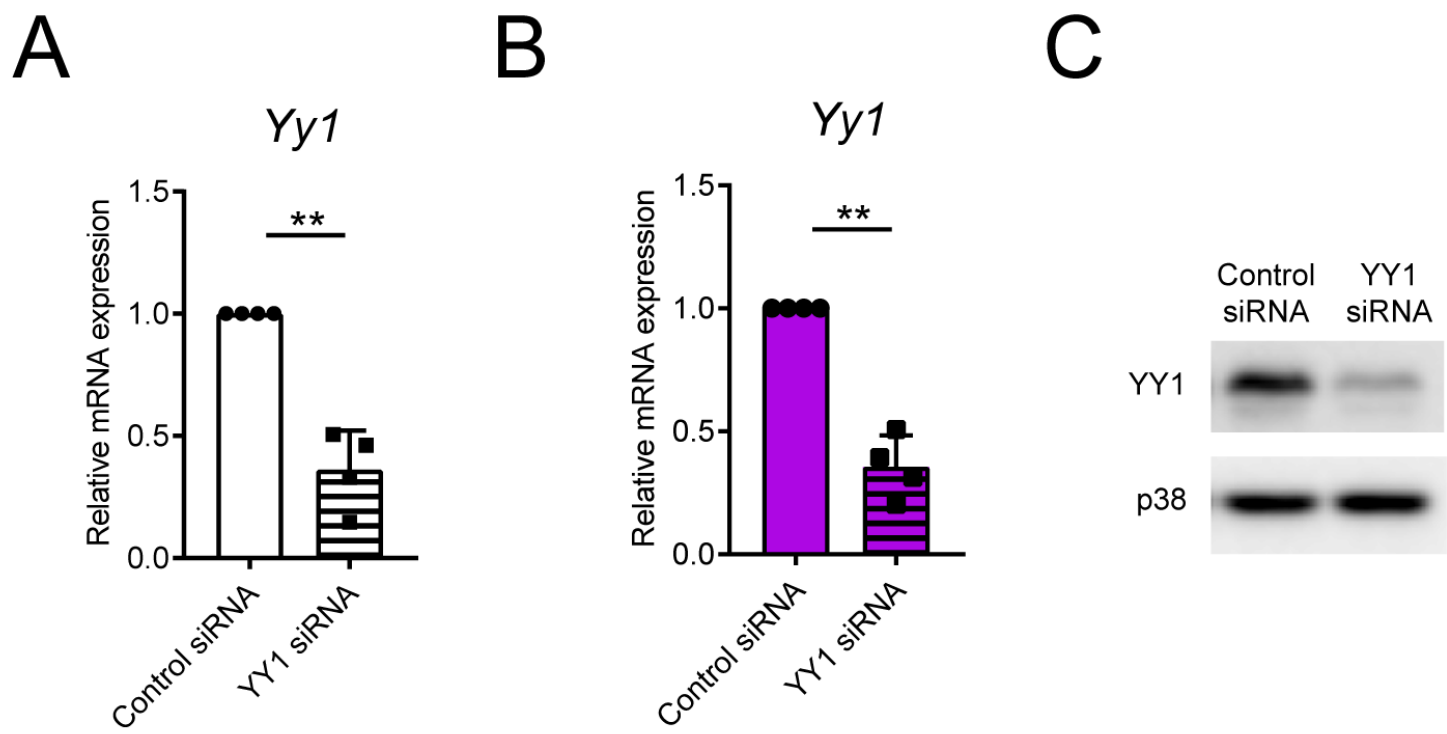
A



B

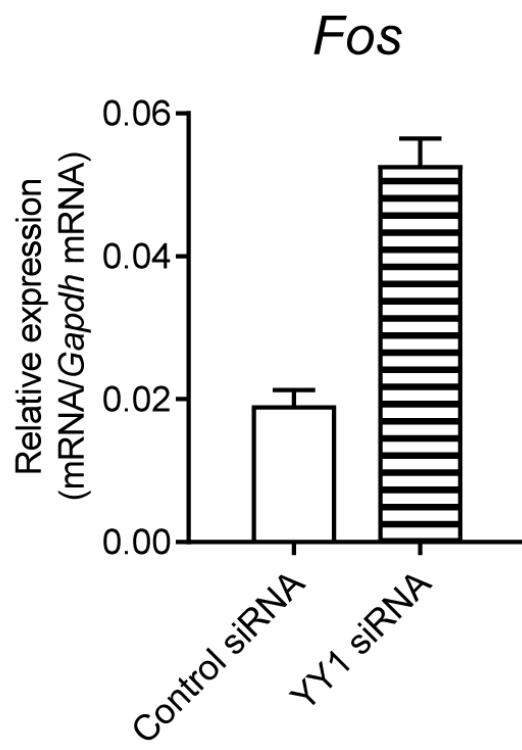


Zhang *et al.* Figure 6-figure supplement 1



Zhang *et al.* Figure 6-figure supplement 2

A



B

